NASA TECHNICAL NOTE

NASA TN D-6772

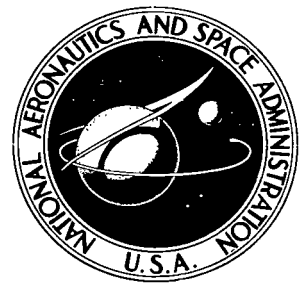

OPTIMUM MASS-STRENGTH ANALYSIS FOR ORTHOTROPIC RING-STIFFENED CYLINDERS UNDER AXIAL COMPRESSION

by John L. Shideler, Melvin S. Anderson, and L. Robert Jackson

Langley Research Center
Hampton, Va. 23365

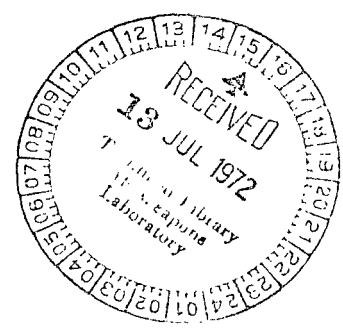

NATIONAL AERONAUTICS AND SPACE ADMINISTRATION • WASHINGTON, D. C. • JULY 1972

1. Report No. NASA TN D-6772	2. Government Accession No.	3. Recipient's Catalog No.
4. Title and Subtitle OPTIMUM MASS-STRENGTH ANALYSIS FOR ORTHOTROPIC RING-STIFFENED CYLINDERS UNDER AXIAL COMPRESSION		5. Report Date June 1972 6. Performing Organization Code
7. Author(s) John L. Shideler, Melvin S. Anderson, and L. Robert Jackson		8. Performing Organization Report No. L-7060 10. Work Unit No. 134-14-08-01
9. Performing Organization Name and Address NASA Langley Research Center Hampton, Va. 23365		11. Contract or Grant No. 13. Type of Report and Period Covered Technical Note
12. Sponsoring Agency Name and Address National Aeronautics and Space Administration Washington, D.C. 20546		14. Sponsoring Agency Code
15. Supplementary Notes		

16. Abstract

An analysis was developed to calculate the minimum mass-strength curve for an orthotropic cylinder subjected to axial compressive loading. The analysis, which includes the effects of ring and stringer eccentricities, is in a general form so that various cylinder wall and stiffener geometries can be considered. Several different ring-stiffened orthotropic configurations were studied. The minimum mass-strength curves and the dimensions associated with these curves are presented for (in order of decreasing efficiency) a tubular double bead, a nonsymmetric double bead, a Z-stiffened skin, and a trapezoidal corrugation. A comparison of efficiencies of the configurations shows a tubular element cylinder to be more efficient than a 3-percent core-density honeycomb-sandwich cylinder. It was found that for an optimized Z-stiffened skin, the location of the Z-stiffeners (internal or external) made a negligible difference in efficiency.

17. Key Words (Suggested by Author(s)) Cylinder Ring stiffened Orthotropic Eccentricity Buckling Minimum weight	18. Distribution Statement Unclassified – Unlimited

19. Security Classif. (of this report) Unclassified	20. Security Classif. (of this page) Unclassified	21. No. of Pages 54	22. Price* $3.00

*For sale by the National Technical Information Service, Springfield, Virginia 22151

OPTIMUM MASS-STRENGTH ANALYSIS FOR ORTHOTROPIC RING-STIFFENED CYLINDERS UNDER AXIAL COMPRESSION

By John L. Shideler, Melvin S. Anderson,
and L. Robert Jackson
Langley Research Center

SUMMARY

Minimizing the structural mass of shell structures has become a more important design consideration as the size of flight structures has increased. Large structures are often lightly loaded, and failure frequently is the result of buckling rather than of yielding. Previous studies have indicated the need to include the effects of stiffener eccentricity for accurate stability analyses of stiffened shells. Each of these efficiency studies has usually been directed toward a single type of construction such as a sandwich, a corrugation, or a skin stiffened with rectangular stringers.

An analysis was developed in this paper to calculate the minimum mass-strength curve for an orthotropic cylinder subjected to axial compressive loading. The analysis is in a general form so that various cylinder wall and stiffener geometries can be considered. It is based on small-deflection stability theory for orthotropic cylinders including the effects of longitudinal and circumferential stiffener eccentricity. It is also based on the generally accepted premise that minimum mass proportions are achieved when all possible structural buckling modes (general, panel, and local) occur at the same applied stress.

Several potentially efficient stiffened cylindrical configurations are studied. The minimum mass-strength curves and the dimensions associated with these curves are presented for (in order of decreasing efficiency) a tubular double bead, a nonsymmetric double bead, a Z-stiffened skin, and a trapezoidal corrugation.

The most efficient configuration studied, the tubular double bead, was, at a loading condition near the yield stress, as efficient as a 3-percent-core-density honeycomb sandwich; and at lesser loadings, it was more efficient than the sandwich. The high efficiency of the two configurations which have curved elements is attributed primarily to the high buckling load associated with a curved element as compared with a flat element. Of the two configurations with flat local elements, the Z-stiffened skin was more efficient than the trapezoidal corrugation, even though, as a column, the trapezoidal corrugation is more efficient. It was found that for the optimized Z-stiffened skin, the location of the Z-stiffeners (internal or external) made a negligible difference in efficiency. All configurations were found to be more efficient with external rings than with internal rings.

INTRODUCTION

Minimizing the mass of shell structures has become a more important design consideration as the size of flight structures has increased. Large structures are often lightly loaded, and failure is frequently the result of buckling rather than of yielding. A historical review of studies aimed at the optimum design of stiffened cylinders is included in reference 1. Studies subsequent to reference 1 (for example, refs. 2 to 4) have emphasized the need for accurate stability analyses of stiffened cylinders to include the effects of stiffener eccentricity. Each of these efficiency studies has usually been directed toward a single type of construction such as sandwich, corrugation, or a skin stiffened with rectangular stringers.

In the present paper a general mass-strength optimization analysis applicable to compressively loaded circular cylinders with various types of orthotropic wall construction is presented. The results are used to assess the efficiency of some recently developed panel configurations (ref. 5) when applied to shell structures including the requirements for ring stiffening. The analysis is based on small-deflection stability theory for orthotropic cylinders (ref. 6) and includes the effects of longitudinal and circumferential stiffener eccentricity. It is also based on the generally accepted premise that minimum mass proportions are achieved when all possible structural buckling modes (general, panel, and local) occur at the same applied stress. (See, for example, refs. 1 and 2.) The efficiencies of these recently developed configurations are compared with those for Z-stiffened and honeycomb construction, and the dimensions of the resulting minimum-mass designs are given as a function of a structural index.

SYMBOLS

The units for the physical quantities defined in this paper are given both in the International System of Units (SI) and in the U.S. Customary Units. The measurements and calculations were made in U.S. Customary Units. Appendix A presents factors relating these two systems of units.

A_1, A_2 terms defined in equations (1) and (8), respectively

A_r, A_s cross-sectional area of ring and of stringer, respectively

A_{rf} cross-sectional flange area of ring

a dimension of cylinder wall (see fig. 2(a))

b	characteristic dimension of element of cylinder wall
b_f, b_w	dimension of Z flange and web, respectively (see fig. 2(b))
b_{1g}, b_{2g}, b_{3g}	terms in general cylinder buckling equation (see eq. (1))
b_{1p}, b_{2p}, b_{3p}	terms in equation for cylinder buckling between rings (see eq. (8))
D_x, D_y, D_{xy}	plate bending and twisting stiffnesses of orthotropic wall
d	stringer spacing
d_x, d_y, d_{xy}	total bending and twisting stiffnesses of cylindrical element (wall + rings)
E_x, E_y	extensional stiffnesses of orthotropic wall
E_o	Young's modulus of orthotropic wall
E_r, E_s	Young's modulus of ring and stringer, respectively
e_x, e_y	total extensional stiffnesses of cylindrical element (wall + rings)
F_s	shape factor defined in equation (7)
G_r, G_s	shear modulus of ring and stringer, respectively
G_{xy}	shear stiffness of orthotropic wall
g_{xy}	shear stiffness term defined after equation (1)
h	sandwich core height
h_r, h_s	height of ring and stringer, respectively
I_r, I_s	moment of inertia of ring and stringer, respectively, about its centroid
i	term defined in equation (1)
J_r, J_s	torsional constant for ring and stringer, respectively

K_1	ratio of axial extensional stiffness of characteristic local element to total axial extensional stiffness, $E_o t_b/e_x$
K_2	coefficient in local buckling equation, $\sigma_{cr} = K_2\left(\frac{t}{b}\right)^n$
K_b	term used to define local buckling coefficient
k_r	ratio of cross-sectional area of attached flange to total cross-sectional flange area of ring (see fig. 2(e))
L	cylinder length (see fig. 1)
ℓ	ring spacing
M	mass
m_g, m_p	number of half waves in cylinder buckle pattern in longitudinal direction for general and panel instability, respectively
N_x	applied compressive load in axial direction
n	exponent in local buckling equation, $\sigma_{cr} = K_2\left(\frac{t}{b}\right)^n$
n_g, n_p	number of full waves in cylinder buckling pattern in circumferential directions for general and panel instability, respectively
P	pitch of orthotropic wall (see fig. 2(c))
R	radius of cylinder to centroid of wall (see fig. 1)
t	thickness
$\bar{t}$	equivalent thickness of cylinder
t_a	thickness of orthotropic wall (see fig. 2(a))
t_b	thickness of characteristic element of orthotropic wall
t_f, t_w, t_s	thickness of Z flange, web, and skin, respectively (see fig. 2(b))

t_{rw} thickness of ring web

$\bar{t}_x$ equivalent thickness of orthotropic wall

V_1, V_2, V_3 ring stiffness terms defined after equation (8)

$\bar{y}$ distance from centroid of orthotropic wall to stiffener attachment surface

$\bar{y}_r$ distance from centroid of ring to ring attachment surface

$\bar{y}_s$ distance from centroid of stringer to stringer attachment surface

$\overline{Z}_r$ distance from centroid of orthotropic wall to centroid of ring, positive for external ring, negative for internal ring

$\overline{Z}_s$ distance from centroid of orthotropic wall to centroid of stringer, positive for external stringer, negative for internal stringer

α term defined after equation (5), $\frac{\bar{t}_x E_o}{E_x}$

β_g general buckling mode shape parameter, $\frac{n_g L}{m_g \pi R}$

β_p panel buckling (buckling between rings) mode shape parameter, $\frac{n_p \ell}{m_p \pi R}$

γ_o density of orthotropic wall material

$\gamma_r \gamma_s$ density of ring and stringer, respectively

ϵ_r, ϵ_s ring and stringer eccentricity terms defined in equation (1)

θ angle of trapezoidal corrugation (see fig. 2(a))

θ_a, θ_b angles of outer and inner bead, respectively (see figs. 2(c) and 2(d))

λ term defined in equation (4)

μ Poisson's ratio

μ_x, μ_y Poisson's ratios for bending of orthotropic plate in axial and circumferential direction, respectively

μ'_x,μ'_y	Poisson's ratios for extension of orthotropic plate in axial and circumferential direction, respectively
σ	stress
σ_y	yield stress
σ_{cr}	local buckling stress
φ_g	general buckling term defined in equation (2)
φ_p	panel buckling (buckling between rings) term defined in equation (8)

Subscripts:

opt	optimum
ring	ring
shell	shell
T	total

ANALYSIS

Theory

An equation relating the mass and strength of an orthotropic cylinder subjected to axial compression can be derived by incorporating an expression for the mass of the cylinder with the simultaneous solution of equations governing general buckling, buckling between rings, and local buckling of the principal load-bearing element of the cylinder wall. Solution of the resulting equation and optimization with respect to the cylinder geometry results in a mass-strength equation which represents the least mass necessary to carry a given load.

A typical stiffened cylinder (shown in fig. 1) consists of a curved orthotropic plate section stiffened with rings. The analysis is based on the following assumptions: The cylinder wall is formed from an orthotropic plate which is characterized by elements subject to local buckling. The moment of inertia of the wall is proportional to a length squared times thickness, that is, proportional to b^2t_b where $b \gg t_b$ and the local buckling stress is proportional to $(t_b/b)^n$. The rings and stringers are spaced closely so that their elastic properties can be averaged over the stiffener spacing for calculation of general buckling.

Derivation of Parameters

The general buckling equation for a stiffened orthotropic cylinder (fig. 1) which includes the effects of stiffener eccentricity is given in reference 6 and can be written as

$$\frac{N_x R}{\sqrt{e_y d_x}} = b_{1g} n_g^2 + \frac{b_{2g}}{n_g^2} + b_{3g} \tag{1}$$

where

$$b_{1g} = \frac{\sqrt{d_x/e_y}}{\beta_g^2 R}\left\{1 + \frac{d_{xy}}{d_x}\beta_g^2 + \frac{d_y}{d_x}\beta_g^4 + \frac{\epsilon_r^2 \beta_g^4}{A_1}\left[\frac{A_1}{\frac{E_x}{e_y}\left(\frac{E_r A_r}{\ell E_x}\right)} - \beta_g^2\left(\frac{e_x}{e_y} + g_{xy}\beta_g^2\right)\right]\right.$$

$$\left. + \frac{\epsilon_s^2}{A_1}\left[\frac{A_1}{\frac{E_x}{e_y}\left(\frac{E_s A_s}{d E_x}\right)} - \left(g_{xy} + \beta_g^2\right)\right] + \frac{2\beta_g^4}{A_1}\epsilon_r \epsilon_s\left(i + g_{xy}\right)\right\}$$

$$b_{2g} = \frac{\beta_g^2 R}{\sqrt{d_x/e_y}}\left[\frac{g_{xy}\left(\frac{e_x}{e_y} - i^2\right)}{A_1}\right]$$

$$b_{3g} = \frac{2g_{xy}}{A_1}\left[\beta_g^2 \epsilon_r\left(\frac{e_x}{e_y} - i\beta_g^2\right) + \epsilon_s\left(\beta_g^2 - i\right)\right]$$

$$A_1 = \left(\frac{e_x}{e_y} + g_{xy}\beta_g^2\right)\left(g_{xy} + \beta_g^2\right) - \beta_g^2\left(i + g_{xy}\right)^2$$

$$\beta_g = \frac{n_g L}{m_g \pi R}$$

$$e_x = E_x\left(\frac{1}{1 - \mu_x'\mu_y'} + \frac{E_s A_s}{d E_x}\right)$$

$$e_y = E_x\left[\frac{E_y}{\left(1 - \mu_x'\mu_y'\right)E_x} + \frac{E_r A_r}{\ell E_x}\right]$$

$$d_x = D_x\left(\frac{1}{1 - \mu_x\mu_y} + \frac{E_sI_s}{dD_x}\right)$$

$$d_y = D_x\left[\frac{D_y}{(1 - \mu_x\mu_y)D_x} + \frac{E_rI_r}{\ell D_x}\right]$$

$$d_{xy} = D_x\left(\frac{2\mu_y}{1 - \mu_x\mu_y} + 2\,\frac{D_{xy}}{D_x} + \frac{G_rJ_r}{\ell D_x} + \frac{G_sJ_s}{dD_x}\right)$$

$$g_{xy} = \frac{G_{xy}}{e_y}$$

$$i = \frac{E_x}{e_y}\left(\frac{\mu_y'}{1 - \mu_x'\mu_y'}\right)$$

$$\epsilon_r = \frac{E_x}{e_y}\left(\frac{E_rA_r}{\ell E_x}\right)\frac{\overline{Z}_r}{\sqrt{d_x/e_y}}$$

$$\epsilon_s = \frac{E_x}{e_y}\,\frac{E_sA_s}{dE_x}\,\frac{\overline{Z}_s}{\sqrt{d_x/e_y}}$$

The buckling load given by equation (1) must be minimized with respect to the number of circumferential waves n_g and the number of longitudinal half waves m_g. If there are many circumferential and longitudinal waves, minimization may be accomplished by setting the derivative of N_x with respect to n_g equal to zero and numerically determining the minimum with respect to β_g. This procedure will give conservative results for short cylinders. The first operation results in

$$\frac{N_xR}{\sqrt{e_yd_x}} = 2\sqrt{b_{1g}b_{2g}} + b_{3g} = \varphi_g \tag{2}$$

As $\beta_g{}^2$ approaches ∞, equation (2) becomes

$$\varphi_{g\left(\beta_g{}^2 \to \infty\right)} = 2\sqrt{\left(\frac{e_x}{e_y} - i^2\right)\left[\frac{d_y}{d_x} + \epsilon_r{}^2\left(\frac{e_y}{E_x\,\frac{E_rA_r}{\ell E_x}} - 1\right)\right]} - 2i\epsilon_r \tag{3}$$

The minimum value of φ_g with respect to β_g^2 was determined by an inspection and search technique by using equation (2) to calculate φ_g for the range $0 < \beta_g^2 < 3 \times 10^5$, and equation (3) to calculate φ_g for $\beta_g^2 \to \infty$. The minimum value of φ_g was determined to within ±0.01 percent with the use of a digital computer.

Equation (2) can be written in terms of the nondimensional structural loading index N_x/E_oR as

$$\frac{N_x}{E_oR} = \frac{\varphi_g}{e_x/E_ob}\left(\frac{e_x}{E_oR}\right)^2\sqrt{\frac{\lambda}{e_x/e_y}} \tag{4}$$

where $\lambda = d_x/e_xb^2$ and b is a characteristic dimension of the cylinder wall upon which local buckling of the wall is based. The term e_x/E_oR is a general form of the expression t/R which controls general buckling; and e_x/E_ob is a general form of t/b which controls local buckling. The mass parameter $\bar{t}/R$ can be introduced through the expression e_x/E_oR, and e_x/E_ob can be eliminated by a local buckling constraint. The effective $\bar{t}$ of an orthotropic cylinder can be written as

$$\frac{\bar{t}}{R} = \frac{e_x}{E_oR}\left(\alpha\frac{E_x}{e_x} + \frac{A_rE_o\gamma_r}{\ell e_x\gamma_o} + \frac{A_sE_o\gamma_s}{de_x\gamma_o}\right) \tag{5a}$$

or

$$\frac{e_x}{E_oR} = \frac{\bar{t}/R}{\alpha\frac{E_x}{e_x} + \frac{A_rE_o\gamma_r}{\ell e_x\gamma_o} + \frac{A_sE_o\gamma_s}{de_x\gamma_o}} \tag{5b}$$

where $\alpha = \bar{t}_xE_o/E_x$ and is used to account for any wall material which does not contribute to E_x. If all the wall material carries axial load and thus contributes to the extensional stiffness E_x, then $\alpha = 1$.

The buckling equation for a characteristic element of the wall can be written as

$$\sigma_{cr} = K_2E_o\left(\frac{t_b}{b}\right)^n$$

The stress due to the applied load is $\sigma = \frac{N_xE_o}{E_x}$. Combining these equations yields

$$\frac{e_x}{E_ob} = \frac{1}{K_1}\left[\frac{N_x\left(\alpha + \frac{E_rA_rE_o\gamma_r}{\ell E_xE_r\gamma_o} + \frac{E_sA_sE_o\gamma_s}{\ell E_xE_s\gamma_o}\right)}{K_2E_o\bar{t}}\right]^{1/n} \tag{6}$$

where $K_1 = E_o t_b / e_x$ is the ratio of axial extensional stiffness of the characteristic local element to the total axial extensional stiffness, and K_2 is the buckling coefficient of the element. Combining equations (5) and (6) with equation (4) results in

$$\frac{\bar{t}}{R} = \frac{\left(\frac{N_x}{E_o R}\right)^{\frac{n+1}{2n+1}}}{F_s} \tag{7}$$

where

$$F_s = \frac{(K_2)^{\frac{1}{2n+1}} \left(\varphi_g K_1 \sqrt{\frac{\lambda}{e_x/e_y}}\right)^{\frac{n}{2n+1}}}{\left(\frac{E_x}{e_x}\right)^{\frac{2n}{2n+1}} \left(\alpha + \frac{E_r A_r}{\ell E_x} \frac{E_o}{E_r} \frac{\gamma_r}{\gamma_o} + \frac{E_s A_s}{d E_x} \frac{E_o}{E_s} \frac{\gamma_s}{\gamma_o}\right)}$$

Equation (7) is a mass-strength expression which relates $\bar{t}/R$ to the structural index $N_x/E_o R$ through the constraint that the local buckling load of the element b equals the general buckling load of the cylinder. However, to determine the most efficient value for the shape factor F_s, the effect of panel buckling (that is, buckling of the cylinder between rings) must be included. The same buckling equation (eq. (15) of ref. 6) can be used to determine the panel buckling load if the cylinder length is taken to be the ring spacing, if the ring terms are removed from the equation, and if the longitudinal mode number is taken equal to unity, that is, $m_p = 1$. The panel buckling equation is then

$$\frac{N_x R}{\sqrt{e_y d_x}} = \pi^2 \frac{R}{\ell^2} \sqrt{\frac{d_x}{e_y}}\, b_{1p} + \frac{b_{2p}}{\pi^2 \frac{R}{\ell^2} \sqrt{\frac{d_x}{e_y}}} + b_{3p} = \varphi_p \tag{8}$$

where

$$b_{1p} = 1 + \beta_p{}^2 \left(\frac{d_{xy}}{d_x} - V_2\right) + \beta_p{}^4 \left(\frac{d_y}{d_x} - V_3\right) + \epsilon_s{}^2 \left\{ \frac{1}{\frac{E_x}{e_y} \frac{E_s A_s}{d E_x}} - \frac{\left[g_{xy} + \beta_p{}^2 (1 - V_1)\right]}{A_2} \right\}$$

$$b_{2p} = (1 - V_1) + \frac{2\beta_p{}^2 i (i + g_{xy})(1 - V_1) - i^2 \left[g_{xy} + \beta_p{}^2 (1 - V_1)\right] - \beta_p{}^2 \left(\frac{e_x}{e_y} + \beta_p{}^2 g_{xy}\right)(1 - V_1)^2}{A_2}$$

$$b_{3p} = 2\epsilon_s \frac{\beta_p^2(i + g_{xy})(1 - V_1) - i\left[g_{xy} + \beta_p^2(1 - V_1)\right]}{A_2}$$

$$\frac{R}{\ell^2}\sqrt{\frac{d_x}{e_y}} = \left(\frac{E_r A_r}{\ell E_x}\right)^2\left(\frac{E_o}{E_r}\right)^2 \frac{\left(\frac{E_x}{e_x}\right)^2\left(\frac{h_r}{t_{rw}}\right)^2}{\left(\frac{A_r}{h_r t_{rw}}\right)^2\left(\frac{h_r}{b}\right)^4}\sqrt{\lambda\frac{e_x}{e_y}}\,\frac{\left(\frac{e_x}{E_o b}\right)^3}{e_x/E_o R}$$

and

$$\beta_p = \frac{n_p \ell}{\pi R}$$

$$V_1 = \frac{E_r A_r}{\ell E_x}\frac{E_x}{e_y}$$

$$V_2 = \frac{G_r J_r}{\ell D_x}\frac{D_x}{d_x}$$

$$V_3 = \frac{E_r I_r}{\ell D_x}\frac{D_x}{d_x}$$

$$A_2 = \left(\frac{e_x}{e_y} + g_{xy}\beta_p^2\right)\left[g_{xy} + \beta_p^2(1 - V_1)\right] - \beta_p^2(i + g_{xy})^2$$

The form of this equation is dictated by the desire to use the same general parameters that appeared in the general buckling equation. By the use of equations (5), (6), and (7), $\frac{R}{\ell^2}\sqrt{\frac{d_x}{e_y}}$ can be expressed as a function of $\bar{t}/R$. Thus,

$$\frac{R}{\ell^2}\sqrt{\frac{d_x}{e_y}} = \left(\frac{E_r A_r}{\ell E_x}\right)^2\left(\frac{E_o}{E_r}\right)^2\left(\frac{h_r}{t_{rw}}\right)^2 \frac{\left(\frac{E_x}{e_x}\right)^{\frac{3(n-1)}{n+1}}\lambda^{\frac{n+4}{2(n+1)}}}{\left(\frac{A_r}{h_r t_{rw}}\right)^2\left(\frac{h_r}{b}\right)^4 (K_1)^{\frac{3n}{n+1}}\left(\frac{e_x}{e_y}\right)^{\frac{2-n}{2(n+1)}}}\left(\frac{\varphi_g}{K_2}\right)^{\frac{3}{n+1}}\left(\alpha + \frac{\bar{t}/R}{\frac{E_r A_r}{\ell E_x}\frac{E_o}{E_r}\frac{\gamma_r}{\gamma_o} + \frac{E_s A_s}{dE_x}\frac{E_o}{E_s}\frac{\gamma_s}{\gamma_o}}\right)^{\frac{2-n}{n+1}} \tag{9}$$

Thus φ_p, and therefore the panel buckling load, can be calculated by selecting a value of the parameter $\bar{t}/R$ and then minimizing equation (8) with respect to β_p^2.

(If $n = 2$, the solution is independent of $\bar{t}/R$, and F_s is constant along any given mass-strength curve.) The minimum φ_p was determined from equation (8) by the method previously described for determining φ_g and using $\varphi_{p\,(\beta_p^2 \to \infty)} = \frac{\pi^2 R}{\ell}\sqrt{\frac{d_x}{e_y}}\left(1 + \frac{\epsilon_s^2}{\frac{E_x}{e_y}\frac{E_s A_s}{dE_x}}\right)$.

Optimization of the mass-strength expression for the cylinder structure requires that the general buckling load equal the panel buckling load. A single value of the parameter h_r/b exists which will satisfy this requirement. A computerized trial-and-error technique was used to determine the value of h_r/b which satisfies $\varphi_g = \varphi_p$. The use of this value of h_r/b and the corresponding φ_g in equation (7) results in an optimum mass-strength expression.

It should be noted that because Donnell-type assumptions are used in deriving the buckling equations (see ref. 6), this analysis is accurate only for n_g equal to zero and for n_g greater than approximately 2. Thus, the validity of results from the mass-strength analysis must be assessed by determining the value of n_g. From the development of equation (2) and by expressing n_g as a function of $\bar{t}/R$ from equations (5) and (7), n_g can be written as

$$n_g = \frac{\left(\beta_g^2\sqrt{\frac{b'_{2g}}{b'_{1g}}}\right)^{1/2}\left(\frac{E_x}{e_x}\right)^{\frac{n-1}{2(n+1)}}\left(\frac{\varphi_g}{K_2}\right)^{\frac{1}{2(n+1)}}}{\left(K_1\sqrt{\lambda}\right)^{\frac{n}{2(n+1)}}\left(\frac{e_x}{e_y}\right)^{\frac{n+2}{4(n+1)}}}\left(\frac{\alpha + \frac{E_r A_r}{\ell E_x}\frac{E_o}{E_r}\frac{\gamma_r}{\gamma_o} + \frac{E_s A_s}{dE_x}\frac{E_o}{E_s}\frac{\gamma_s}{\gamma_o}}{\bar{t}/R}\right)^{\frac{n}{2(n+1)}} \tag{10}$$

where

$$b'_{1g} = b_{1g}\frac{R\beta_g^2}{\sqrt{d_x/e_y}}$$

and

$$b'_{2g} = b_{2g}\frac{\sqrt{d_x/e_y}}{R\beta_g^2}$$

Significant Stiffness Ratios

For a selected ring and panel configuration, every stiffness ratio in the mass-strength analysis (eq. (7) constrained by the condition $\varphi_g = \varphi_p$) can be calculated as a function of a few design variables. These ratios along with some required quantities are as follows:

(a) Wall	
$\frac{d_{xy}}{d_x}$	$\frac{\mu'_y}{1 - \mu'_x\mu'_y}$
$\frac{d_y}{d_x}$	$\frac{\bar{y}}{\sqrt{d_x/e_y}}$
$\frac{D_x}{d_x}$	
$\frac{E_x}{e_x}$	α
	n
$\frac{E_x}{e_y}$	λ
$\frac{e_x}{e_y}$	K_1
g_{xy}	K_2

(b) Rings
$\frac{E_r A_r}{\ell E_x}$
$\frac{E_r I_r}{\ell D_x}$
$\frac{\bar{y}_r}{\sqrt{d_x/e_y}}$
$\frac{G_r J_r}{\ell D_x}$
$\frac{A_r}{h_r t_{rw}}$

(c) Stringer
$\frac{E_s A_s}{dE_x}$
$\frac{E_s I_s}{dD_x}$
$\frac{\bar{y}_s}{\sqrt{d_x/e_y}}$
$\frac{G_s J_s}{dE_x}$

The task of minimizing mass becomes a minimization with respect to only a few design variables. The design variables associated with each configuration studied in this paper are discussed in the next section.

RESULTS AND DISCUSSION

The analysis presented in this paper was applied to several potentially efficient ring-stiffened cylinders subjected to axial compression. The wall configurations were (1) trapezoidal corrugation, (2) Z-stiffened skin, and (3) double bead; these configurations are shown in figure 2. The design variables for these configurations are presented in appendixes B, C, and D. Figure 2 shows a T-section ring which is the type of ring arbitrarily selected for use with each configuration. The ring can be described by the five stiffness ratios given in the preceding section which relate ring properties to cylinder wall properties. The selection of one of these ratios as a design variable will size the ring with respect to the wall. In this paper, the ring area ratio $E_r A_r/\ell E_x$ was selected to be this design variable. The remaining four ring stiffness ratios can be calculated from the other design variables used for the T-ring, A_{rf}/A_r, k_r, and h_r/t_{rw}. It was assumed that $G_r J_r/\ell E_x = 0$ for the open-section T-ring. In general, there is no loading requirement in the ring which would determine a web depth to thickness ratio h_r/t_{rw}. It is more efficient to use a large value of h_r/t_{rw}; consequently, a value of $h_r/t_{rw} = 80$ was arbitrarily selected as a maximum practical design value as was done in reference 3. The ring geometric parameter k_r was limited to values between 0.2 and 0.8 in an attempt to provide sufficient flange material to stabilize the ring web.

No configuration was allowed to carry a stress greater than the material yield stress because most buckling failures occur at a stress below or near the yield stress where the tangent and secant moduli are decreasing rapidly. A value of $\sigma_y/E_o = 0.005$ is representative of many materials and was used in this study to define the yield stress.

Trapezoidal Corrugation

The parameters which were used to describe the trapezoidal corrugation (fig. 2(a)) are listed in appendix B. Two of the design variables, a/b and θ, were varied to determine the geometry which results in the greatest efficiency. The parameter t_a/t_b was assumed to be equal to 1.0 which would be the case for common fabrication processes although reference 5 indicated that for a flat plate, $t_a/t_b = 1.1$ is optimum. Values used for K_b in determining the local buckling coefficient K_2 are a function of a/b and were obtained from figure 9(c) of reference 7. The general terms used in the mass-strength analysis are given in appendix B.

The results are presented in figure 3. The optimum mass-strength curve, the optimum dimensions, and the average stress for the corrugation are shown as a function of the structural index N_x/E_oR. The dimensions for the cylinder can be obtained from equations presented in appendix B. Values for curves presented in figure 3 and the optimum values of the wall and ring parameters which were varied are presented in table I(a). It can be seen from the figure that the mass, stress, and optimum dimensions increase linearly on a log-log plot with increasing structural index until the yield stress is reached. For greater values of N_x/E_oR, the stress was held constant, and the mass increases at a greater rate. In the linear part of the curves, the depth of the rings is about three times the height of the corrugation for internal rings and 2.6 times the corrugation height for external rings. Over the range of structural index from 3×10^{-7} to 3×10^{-6}, which approximates the range of interest for large aircraft and launch vehicles, the optimum ring spacing varies from about $\ell/R = 0.2$ to $\ell/R = 0.3$ for internal rings and from $\ell/R = 0.13$ to $\ell/R = 0.22$ for external rings.

The trapezoidal corrugation is about 25 percent heavier with internal rings than with external rings. For the case with internal rings, the optimum corrugation angle is $56^o \pm 1^o$, the ring material is 32 ± 1 percent of the mass of the corrugation. For the case with external rings, the optimum corrugation angle is $58^o \pm 1^o$ and the ring material is 25 percent of the mass of the corrugation. The values shown for A_{rf}/A_r and k_r for external rings in table I(a) satisfy the inequality $E_rI_r/\ell D_x > E_rA_r/\ell E_x$, a condition which results in an axisymmetric buckling mode ($n_g = 0$ and $\varphi_g = 2.0$; see ref. 3). Other values of A_{rf}/A_r and k_r will not change the mass-strength results as long as this inequality is satisfied and $E_y = 0$. Hence, for external rings, $A_{rf}/A_r = 0.65$, $k_r = 0.8$ are reasonable values which satisfy the inequality, but they are not the only values which do so.

These results are in very good agreement with those of reference 3 except that the optimum value of $E_rA_r/\ell E_x$ for external rings was found to be one-fourth as compared with one-third in reference 3. The value one-third was obtained by optimizing the shape

factor with respect to $E_r A_r/\ell E_x$ without eliminating b/t. However, b/t is a function of $E_r A_r/\ell E_x$, and if b/t is eliminated prior to optimization, the correct value $E_r A_r/\ell E_x = 1/4$ results.

Z-Stiffened Skin

The Z-stiffened skin shown in figure 2(b) is a commonly used type of aerospace structure. The attachment of rings to the skin provides a convenient method for stopping crack propagation but requires many cutouts in the ring webs to allow for the Z-stiffeners. All three ring attachment locations shown were analyzed, but the effect of ring web cutouts or the need for attachment clips in the case of ring attachment to the stiffeners was not considered.

The parameters which were used to describe the Z-stiffened cylinder are listed in appendix C. For this case, the skin was treated as the cylinder wall. The thickness of the web and flange of the Z-stiffener was assumed to be equal $\left(t_w/t_f = 1\right)$, and the width of each flange was taken equal to 0.4 of the depth $\left(b_f/b_w = 0.4\right)$. This value of b_f/b_w is large enough to prevent lateral deflection of the web. (See ref. 8.) The two variables b_w/d and t_w/t_s were varied to determine the greatest efficiency of the section. Values for the local buckling coefficient K_2 are dependent on the proportions of the composite wall and were determined from reference 8.

The results of the optimization are presented in figures 4(a) and 4(b). The mimimum mass, optimum dimensions, and average stress are plotted as a function of $N_x/E_o R$ for internal and external Z-stiffeners and for internal or external rings. The equations for the dimensions are presented in appendix C. The data points used to determine the curves presented in the figures and the optimum values of the wall and ring parameters which resulted from the analysis are given in table I(b).

Considerably less percentage of ring material (8.4 percent of the total mass) was required for the Z-stiffened skin for internal rings than for the trapezoidal corrugation (24 percent) because the skin contributes an extensional stiffness E_y to the total e_y and thus reduces the extensional stiffness requirement for the rings. The corrugation has negligible E_y.

It has been shown in reference 6 that large differences in efficiency can result when stringers of given geometry are moved from internal to external stiffening without changing their proportions. However, comparison of figures 4(a) and 4(b) shows that the use of internal or external stringers results in about the same efficiency even though the optimum proportions and stresses for the two cases differ. Thus, if the proportions are properly adjusted, little difference in efficiency can be expected between internal or external stringers. However, the use of external rings results in approximately a 10-percent increase in efficiency over internal rings for either internal or external stringers.

Attaching internal rings to internal Z-stiffeners is about 2 percent more efficient than attaching them to the skin. Since this difference in efficiency is small, the selection of the attachment location for internal rings becomes largely influenced by other factors such as fabrication ease, crack propagation, and ring-web cutout constraints. The linear part of the curves (figs. 4(a) and 4(b)) show that the optimum depth of internal rings is about three times the height of the Z-stiffener, but for external rings the ratio is about 4.3 for internal Z-stiffeners and 2.4 for external Z-stiffeners. From a structural index of 3×10^{-7} to 3×10^{-6}, the optimum ring spacing varies from about $\ell/R = 0.07$ to $\ell/R = 0.20$. Ring spacing is about 30 percent greater for external Z-stiffeners than for internal Z-stiffeners.

Longitudinally stiffened cylinders have been studied in reference 9 (hat-section stringers), and reference 10 (T-section stringers). However, optimum ring spacing was not rigorously determined. Shanley criteria were used to size the rings in reference 9, and the ring mass was assumed to be equal to the stringer mass in reference 10. The mass-strength curves for these cylinders are compared in figure 4(c) with the optimum Z-stiffened cylinder. The large improvement in efficiency of the Z-stiffeners over the results of reference 9 is largely due to improvements in the cylinder buckling theory used, namely, the theoretical accounting for the effects of rings instead of using the empirical Shanley criteria and including the effects of eccentricities. (See ref. 6.) Figure 4(c) shows little difference in efficiency between the Z-stiffened cylinder and the T-stiffened cylinder of reference 10. However, the assumption of equal external ring and stringer masses (ref. 10) results in a ring mass about 25 percent of the total mass whereas the comparable Z-stiffened skin has a ring mass only 6.4 percent of the total mass. (The percentage for the Z-stiffened cylinder varies from 4 percent to 15 percent depending on internal or external stiffener and ring location.) Although the total masses for the two designs are comparable, the assumption of equal ring and stringer masses leads to more rings (smaller ring spacing) and increased stresses. (An increase in stress of 25 percent relative to the results of this paper was found for the T-stiffened cylinder of ref. 10.)

Double Bead

The double-bead concepts consist of two sheets that are beaded longitudinally between rings as shown in figures 2(c) and 2(d). These double-beaded configurations have a potential mass-strength advantage over the trapezoidal corrugation and the Z-stiffened skin configuration because a curved element has a higher local buckling stress than a flat element. Two concepts of the double bead were studied. One is a tubular concept $\left(\theta_a/\theta_b = 1\right)$ which may have application to aerodynamically heated flight vehicles with heat-shield-covered surfaces or to vehicles with exposed surfaces where drag is not

critical. The second is a nonsymmetric concept where the outer angle θ_a was reduced to provide a relatively smooth exterior surface for applications where aerodynamic drag is of concern. Because the double bead becomes less efficient as θ_a/θ_b is reduced, the selection of θ_a for application to a particular vehicle would be a trade-off between structural efficiency and aerodynamic performance. This trade-off was not investigated in this paper. The results of reference 11 indicate that $\theta_a = 60^o$ may be sufficient to avoid thermal buckling of the outer skin. Thus, a configuration with $\theta_a = 60^o$ $\left(\theta_a/\theta_b = 1/3\right)$ was selected to be studied to determine the extent of loss of structural efficiency from such a change. If the nonsymmetric configuration is beaded, a moment will exist as a result of the offset between the neutral axis of the bead and the neutral axis of the flat portion where the beads are closed out. This eccentric loading can be avoided if the beads for the nonsymmetric configurations are not closed out at ring attachments but are continuous as for a corrugation. The rings are attached to the inner bead. (See fig. 2(d).)

The parameters which were used to describe the double-beaded cylinder are listed in appendix D. The angle for the interior bead θ_b was taken to be equal to 180^o. The double bead was sized so that the upper and lower beads buckle at the same stress. A value of $b/P = 0.4$ was selected to provide a flat surface between beads for joining and to assure that the flat surface buckles at a stress higher than that for the circular-arc element for the range of structural index greater than 1×10^{-7}. Thus, the configuration had the constraints $a/b = t_a/t_b$ and $b/P = 0.4$, even though $b/P = 0.5$ (corresponding to no flat surface between beads) would be more efficient (ref. 5). Values for the local buckling coefficient $\left(K_2 = 1.75\right)$ and the exponent of the local buckling equation ($n = 1.35$) were taken from reference 5 and are a result of a conservative fit to empirical data given in reference 12.

Figures 5(a) and 5(b) show the optimum mass-strength curve, optimum dimensions, and the associated stress for the tubular and nonsymmetric double bead as a function of the structural index N_x/E_oR. The equations defining these parameters are presented in appendix D. The results presented in the figures and the optimum values of the wall and ring parameters which were varied are tabulated in table I(c). The behavior of the curves is similar to that for the corrugated and Z-stiffened configurations. However, the slope of the mass-strength curve is no longer $(n + 1)/(2n + 1)$ since $n \neq 2$ and φ_p is therefore a function of $\bar{t}/R$. (See eqs. (7), (8), and (9).)

Figure 5(a) illustrates that the use of internal rings with the tubular double bead results in approximately a 10-percent weight increase over that for external rings, the same penalty as for the Z-stiffened configuration. For internal rings, the rings were 12 ± 1 percent of the mass of the double bead, and the percent of the ring material located in the flanges varies from 65 to 75 percent. The optimum value $k_r = 0.8$ was the maximum allowed, as was the case for the corrugation. The optimum ring depth is about

0.75 times the diameter of the tube. Ring spacing varies from about $\ell/R = 0.24$ to $\ell/R = 0.35$ over the range of structural index from 3×10^{-7} to 3×10^{-6}. This ring spacing is greater than that of the corrugated cylinder and more than twice that of the Z-stiffened cylinder. For external rings, the optimum geometry resulted in ring material 22 percent of the mass of the double bead. The eccentricity of the external rings has the same effect on the tubular structure as it has for the corrugation; that is, the geometry of the rings $(A_{rf}/A_r$ and $k_r)$ do not affect the optimum buckling load because the inequality $E_r I_r/\ell D_x > E_r A_r/\ell E_x$ for $E_y = 0$ is satisfied. The ring depth for external rings is about equal to the tube diameter; over this structural index range, the ring spacing varies from about $\ell/R = 0.17$ to $\ell/R = 0.24$.

Figure 5(b) presents results for the nonsymmetric double bead for only internal rings since the reason for considering $\theta_a/\theta_b = 1/3$ was to provide a relatively smooth outer surface – an objective which would be defeated by the use of external rings. It was found that the optimum configuration occurs at values of A_{rf}/A_r and k_r of approximately 0.7 and 0.8, respectively. These values are presented in table I(c). The optimum value of $E_r A_r/\ell E_x$ was 0.18 ± 0.01. The optimum values of ℓ/R cover the same range as for the tubular configuration with internal rings.

Mass-Strength Comparison

A comparison of the mass-strength curves for the configurations studied with internal rings is shown in figure 6(a). An unstiffened skin and a honeycomb sandwich with a core density of 3 percent of the face sheet density are also shown for comparison. The curve for the honeycomb sandwich includes no ring material since none is needed for optimum design; however, an occasional ring may be required at spacings not greater than approximately a radius to serve as formers. The curve for the unstiffened skin also does not include rings but gives an indication of the improvement in efficiency that is achieved by the addition of stiffening.

The tubular configuration appears to be the most efficient configuration over the range of structural index for which $\sigma_y/E < 0.005$. The unsymmetric double bead is about 35 percent heavier than the tubular configuration but does provide a somewhat smoother external surface in exchange for the reduction in structural efficiency. The Z-stiffened skin (internal or external Z-stiffeners) is 45 to 50 percent heavier than the tubular configuration and provides a smooth outer surface. The trapezoidal corrugation is 75 to 80 percent heavier than the tubular configuration and does not have a smooth outer surface. The Z-stiffened skin is lighter than the trapezoidal corrugation even though as a wide column the reverse is true. (See ref. 13.) This difference is attributed to the circumferential extensional stiffness E_y of the Z-stiffened skin which, as mentioned earlier, reduces the ring requirement.

A comparison of the mass-strength curves for the configurations studied with external rings is shown in figure 6(b). The unsymmetric double bead was not included since the tubular double bead is always more efficient and the incentive for a smooth surface is lost if exterior rings are used. As was previously mentioned, the use of external rings has a beneficial effect for each configuration studied. Figure 6(b) shows the configurations to have the same relative order of efficiency as internal rings, but a narrower spread exists between the configurations. The trapezoidal corrugation, which shows the greatest efficiency gain from the use of external rings, is almost as efficient as the Z-stiffened skin. The tubular configuration is about 50 percent lighter than the others except for the 3-percent honeycomb which has nearly equal efficiency in the high range of structural index.

Design Comparison

A comparison of the weight and the dimensions of each configuration when applied to a large cylindrical structure is given in table II. The design conditions (N_x = 350.2 kN/m (2000 lbf/in.), R = 304.8 cm (120 in.)) are typical of lightly loaded shells in flight structures and corresponds to a structural index of $N_x/E_0R = 1.67 \times 10^{-6}$. The configurations are listed in order of increasing mass. The sketches in the table are scaled to indicate the relative sizes of the configurations at this structural index. The range of mass is from 3.28 kg/m^2 (0.67 lbm/ft^2) for the tubular double bead with external rings to 5.96 kg/m^2 (1.22 lbm/ft^2) for the corrugation with internal rings – a range of more than 2.44 kg/m^2 (1/2 lbm/ft^2). The difference between the masses for skins stiffened with internal or external Z-stiffeners is only about 2 percent or less. Note, however, that the skin stiffened with internal Z-stiffeners and external rings is about 10 percent lighter than the skin with external Z-stiffeners and internal rings even though the wall cross sections look very much alike. The table also shows the skin thickness, height, and ring spacing for each configuration. The tubular double bead and the trapezoidal corrugation have the largest ring spacing which is an advantage since nonoptimum factors such as attachments are not included in these masses.

CONCLUSIONS

An analysis was developed to calculate the optimum mass-strength curve for an orthotropic cylinder subjected to axial compressive loading. The analysis is in a general form so that various cylinder wall and stiffener geometries can be considered. The analysis which includes the effects of ring and stiffener eccentricities was used to study several different ring-stiffened geometric configurations. Minimum mass-strength curves and the dimensions associated with these curves are presented for (in order of decreasing efficiency) a tubular double bead, a nonsymmetric double bead, a Z-stiffened

skin, and a trapezoidal corrugation. Comparison of the efficiencies of the configurations leads to the following conclusions:

1. The most efficient configuration studied, the tubular double bead, is, at a loading condition near the yield stress, as efficient as a 3-percent core-density honeycomb sandwich; and at lesser loadings, it is more efficient than the sandwich.

2. The high efficiency of the two configurations which have curved elements is attributed primarily to the high buckling load associated with a curved element as compared with a flat element.

3. Of the two configurations with flat local elements, the Z-stiffened skin is more efficient than the trapezoidal corrugation, even though as a column the trapezoidal corrugation is more efficient.

4. The nonsymmetric double bead is also more efficient than the trapezoidal corrugation and offers a smoother surface.

5. It was found that for the optimized Z-stiffened skin, the location of the Z-stiffeners (internal or external) made a negligible difference in efficiency but that optimum proportions for the two cases differ.

6. All configurations were found to be more efficient with external rings than with internal rings.

Langley Research Center,
National Aeronautics and Space Administration,
Hampton, Va., May 3, 1972.

APPENDIX A

CONVERSION OF U.S. CUSTOMARY UNITS TO SI UNITS

The International System of Units (SI) (ref. 14) was adopted by the Eleventh General Conference on Weights and Measures, Paris, October 1960 in resolution No. 12. Conversion factors for the units used herein are given in the following table:

Physical quantity	U.S. Customary Unit	Conversion factor (*)	SI Unit
Force	pounds force (lbf)	4.448	newtons (N)
Length	inches (in.)	0.0254	meters (m)
Mass	pounds mass (lbm)	0.4536	kilograms (kg)
Load intensity	pounds force/inch (lbf/in.)	175.1	newtons/meter (N/m)
Stress, modulus	pounds force/inch^2 (lbf/in^2)	6894.8	newtons/meter^2 (N/m^2)

*Multiply value given in U.S. Customary Unit by conversion factor to obtain equivalent value in SI Unit.

Prefixes to indicate multiples of units are as follows:

Prefix	Multiple
giga (G)	10^9
mega (M)	10^6
kilo (K)	10^3
centi (c)	10^{-2}

APPENDIX B

TRAPEZOIDAL CORRUGATION

This appendix contains the general terms needed for the mass-strength analysis of a corrugated ring-stiffened cylinder. Also included are the geometric parameters used to describe the wall configuration and optimum dimensions of the configuration expressed as a function of the structural index N_x/E_oR.

The geometry of the trapezoidal corrugation is illustrated in figure 2(a). The dimension and thickness of the characteristic element are designated by b and t_b, respectively. The parameters used to describe this configuration are as follows:

Design variables

$\frac{a}{b}$, varied

θ, varied

$\frac{t_a}{t_b} = 1.0$

Other parameters

$n = 2.0$

$\mu = 0.32$

K_b, function of a/b (see ref. 7)

Expressions for the extensional, bending, and torsional stiffnesses of the corrugation are

$$E_x = \frac{E_o t_b \left(\frac{a}{b}\frac{t_a}{t_b} + 1\right)}{\frac{a}{b} + \cos\theta}$$

$$E_y = D_y = D_{xy} = 0$$

$$D_x = \frac{E_o t_a b^2 \sin^2\theta}{4\frac{t_a}{t_b}} \frac{\frac{a}{b}\frac{t_a}{t_b} + \frac{1}{3}}{\frac{a}{b} + \cos\theta}$$

$$G_{xy} = \frac{E_o t_a \left(\frac{a}{b} + \cos\theta\right)}{2(1+\mu)\left(\frac{a}{b} + \frac{t_a}{t_b}\right)}$$

$$\mu_x = \mu_y = \mu'_x = \mu'_y = 0$$

and the stiffness ratios used in the mass-strength analysis are

$$\frac{e_x}{e_y} = \frac{1}{E_r A_r / \ell E_x}$$

$$g_{xy} = \frac{\left(\frac{a}{b} + \cos\theta\right)^2}{2(1+\mu)\left(\frac{a}{b} + \frac{t_a}{t_b}\right)\left(\frac{a}{b} + \frac{1}{t_a/t_b}\right)\frac{E_r A_r}{\ell E_x}}$$

$$i = 0$$

$$\epsilon_r = \pm\left(\frac{\frac{\bar{y}_r}{h_r} + \frac{\bar{y}}{h_r}}{\frac{\sqrt{d_x/e_y}}{h_r}}\right)$$

where + and - indicate external and internal rings, respectively, and

$$\frac{\bar{y}}{h_r} = \frac{b \sin\theta}{2h_r}$$

$$\frac{\bar{y}_r}{h_r} = (1 - k_r)\frac{A_{rf}}{A_r} + \frac{1}{2\,\frac{A_r}{h_r t_{rw}}}$$

$$\frac{\sqrt{d_x/e_y}}{h_r} = \frac{\sin\theta}{2\,\frac{h_r}{b}}\sqrt{\frac{\frac{a}{b}\frac{t_a}{t_b} + \frac{1}{3}}{\left(\frac{a}{b}\frac{t_a}{t_b} + 1\right)\frac{E_r A_r}{\ell E_x}}}$$

$$\frac{d_{xy}}{d_x} = \frac{E_y}{e_x} = 0$$

$$\frac{d_y}{d_x} = \frac{E_r I_r}{\ell D_x} = \frac{6\left(\frac{h_r}{b}\right)^2 \frac{E_r A_r}{\ell E_x}}{\sin^2\theta}\left\{\frac{A_{rf}}{A_r}\left[(1 - k_r)\left(1 - \frac{\bar{y}_r}{h_r}\right)^2 + k_r\left(\frac{\bar{y}_r}{h_r}\right)^2\right] + \frac{\left(\frac{\bar{y}_r}{h_r}\right)^3 + \left(1 - \frac{\bar{y}_r}{h_r}\right)^3}{3\,\frac{A_r}{h_r t_{rw}}}\right\}$$

$$\frac{E_x}{e_y} = \frac{1}{E_r A_r / \ell E_x}$$

$$\frac{E_x}{e_x} = 1.0$$

$$\alpha = 1.0$$

$$K_1 = \frac{\frac{a}{b} + \cos\theta}{\frac{a}{b}\frac{t_a}{t_b} + 1}$$

$$K_2 = \frac{\pi^2 K_b}{12(1 - \mu^2)}$$

$$\frac{A_r}{h_r t_{rw}} = \frac{1}{1 - \frac{A_{rf}}{A_r}}$$

$$\lambda = \frac{\left(\frac{a}{b}\frac{t_a}{t_b} + \frac{1}{3}\right)\sin^2\theta}{4\left(\frac{a}{b}\frac{t_a}{t_b} + 1\right)}$$

$$\frac{D_x}{d_x} = V_1 = 1.0$$

$$V_2 = \frac{G_r J_r}{\ell D_x}$$

$$V_3 = \frac{E_r I_r}{\ell D_x}$$

The dimensions (normalized by the cylinder radius R) and the local stress can be expressed as a function of the structural index $N_x/E_o R$ as

$$\frac{t_b}{R} = \frac{\frac{a}{b} + \cos\theta}{\left(\frac{a}{b}\frac{t_a}{t_b} + 1\right)\left(\alpha + \frac{E_r A_r}{\ell E_x}\frac{E_o}{E_r}\frac{\gamma_r}{\gamma_o}\right)F_s}\left(\frac{N_x}{E_o R}\right)^{3/5}$$

$$\frac{b}{R} = \frac{K_2^{1/2}\left(\frac{a}{b} + \cos\theta\right)}{\left[\left(\alpha + \frac{E_r A_r}{\ell E_x}\frac{E_o}{E_r}\frac{\gamma_r}{\gamma_o}\right)F_s\right]^{3/2}\left(\frac{a}{b}\frac{t_a}{t_b} + 1\right)}\left(\frac{N_x}{E_o R}\right)^{2/5}$$

$$\frac{h_r}{R} = \frac{\frac{h_r}{b}K_2^{1/2}\left(\frac{a}{b} + \cos\theta\right)}{\left[\left(\alpha + \frac{E_r A_r}{\ell E_x}\frac{E_o}{E_r}\frac{\gamma_r}{\gamma_o}\right)F_s\right]^{3/2}\left(\frac{a}{b}\frac{t_a}{t_b} + 1\right)}\left(\frac{N_x}{E_o R}\right)^{2/5}$$

$$\frac{\ell}{R} = \frac{\left(\frac{a}{b} + \cos\theta\right)^2 K_2 \frac{A_r}{h_r t_{rw}}\left(\frac{h_r}{b}\right)^2\left(\frac{N_x}{E_o R}\right)^{1/5}}{\frac{h_r}{t_{rw}}\frac{E_o}{E_r}\frac{E_r A_r}{\ell E_x}\left(\frac{a}{b}\frac{t_a}{t_b} + 1\right)^2\left[F_s\left(\alpha + \frac{E_r A_r}{\ell E_x}\frac{E_o}{E_r}\frac{\gamma_r}{\gamma_o}\right)\right]^2}$$

$$\frac{A_r}{R^2} = \frac{K_2 \frac{A_r}{h_r t_{rw}}\left(\frac{h_r}{b}\right)^2\left(\frac{a}{b} + \cos\theta\right)^2}{\left[\left(\alpha + \frac{E_r A_r}{\ell E_x}\frac{E_o}{E_r}\frac{\gamma_r}{\gamma_o}\right)F_s\right]^3 \frac{h_r}{t_{rw}}\left(\frac{a}{b}\frac{t_a}{t_b} + 1\right)^2}\left(\frac{N_x}{E_o R}\right)^{4/5}$$

$$\frac{\sigma_{cr}}{E_o} = \left(\alpha + \frac{E_r A_r}{\ell E_x}\frac{E_o}{E_r}\frac{\gamma_r}{\gamma_o}\right)F_s\left(\frac{N_x}{E_o R}\right)^{2/5}$$

APPENDIX C

Z-STIFFENED SKIN

This appendix contains the general terms needed for the mass-strength analysis of a Z-stiffened cylinder with rings. Also included are the geometric parameters used to describe the wall configuration and optimum dimensions of the configuration expressed as a function of the structural index N_x/E_oR.

The geometry of the Z-stiffened skin is illustrated in figure 2(b). The dimension and thickness of the characteristic element of the cylinder wall is d and t_s. The parameters used to describe this configuration are as follows:

Design variables

$\frac{b_w}{d}$, varied

$\frac{t_w}{t_s}$, varied

$\frac{t_w}{t_f} = 1$

$\frac{b_f}{b_w} = 0.4$ (ref. 8)

Other parameters

$n = 2.0$

$\mu = 0.32$

K_b, function of design variables (see ref. 8)

Expressions for the extensional, bending, and torsional stiffnesses of the Z-stiffened skin are

$$E_x = E_o t_s$$

$$E_y = E_o t_s$$

$$G_{xy} = \frac{E_o t_s}{2(1 + \mu)}$$

$$D_x = D_y = D_{xy} = \mu_x = \mu_y = 0$$

$$\mu'_x = \mu'_y = \mu$$

The stiffness ratios used in the mass-strength analysis are

$$\frac{e_x}{e_y} = \frac{\dfrac{1}{1-\mu^2} + \dfrac{E_s A_s}{d E_x}}{\dfrac{1}{1-\mu^2} + \dfrac{E_r A_r}{\ell E_x}}$$

$$g_{xy} = \frac{1}{2(1+\mu)\left(\dfrac{1}{1-\mu^2} + \dfrac{E_r A_r}{\ell E_x}\right)}$$

$$i = \frac{\mu}{1 + (1-\mu^2)\dfrac{E_r A_r}{\ell E_x}}$$

$$\epsilon_r = \frac{E_r A_r / \ell E_x}{\dfrac{1}{1-\mu^2} + \dfrac{E_r A_r}{\ell E_x}} \left(\pm \frac{\overline{Z}_r / h_r}{\sqrt{\dfrac{d_x / e_y}{h_r}}} \right)$$

where + and - indicate external and internal rings, respectively, and

$$\frac{\sqrt{d_x / e_y}}{h_r} = \frac{1}{h_r / d} \sqrt{\frac{\dfrac{t_w}{t_s}\left(\dfrac{b_w}{d}\right)^3 \left(\dfrac{1}{6} + \dfrac{b_f / b_w}{t_w / t_f}\right)}{2\,\dfrac{E_o}{E_s}\left(\dfrac{1}{1-\mu^2} + \dfrac{E_r A_r}{\ell E_x}\right)}}$$

The ring eccentricity parameter $\overline{Z}_r / h_r$ is given in the following table:

Z-stiffener location	$\overline{Z}_r / h_r$			
	Internal rings	Internal rings attached to skin	External rings	External rings attached to skin
Internal	$\dfrac{b_w/d}{h_r/d} + \dfrac{\bar{y}_r}{h_r}$	$\dfrac{\bar{y}_r}{h_r}$		$\dfrac{\bar{y}_r}{h_r}$
External		$\dfrac{\bar{y}_r}{h_r}$	$\dfrac{b_w/d}{h_r/d} + \dfrac{\bar{y}_r}{h_r}$	$\dfrac{\bar{y}_r}{h_r}$

and

$$\frac{\bar{y}_r}{h_r} = (1 - k_r)\frac{A_{rf}}{A_r} + \frac{1}{2\,\dfrac{A_r}{h_r t_{rw}}}$$

$$\frac{d_{xy}}{d_x} = 0$$

$$\frac{d_y}{d_x} = \frac{E_r I_r}{\ell \frac{E_s I_s}{d}} = \frac{2 \frac{E_r A_r}{\ell E_x} \frac{E_o}{E_s} \frac{I_r}{A_r h_r^2} \left(\frac{h_r}{d}\right)^2}{\frac{t_w}{t_s}\left(\frac{b_w}{d}\right)^3 \left(\frac{1}{6} + \frac{b_f/b_w}{t_w/t_f}\right)}$$

(Note that $E_r I_r/\ell D_x$ and $E_s I_s/dD_x$ are undefined since $D_x = 0$.)

where

$$\frac{I_r}{A_r h_r^2} = \frac{A_{rf}}{A_r}\left[(1 - k_r)\left(1 - \frac{\bar{y}_r}{h_r}\right)^2 + k_r\left(\frac{\bar{y}_r}{h_r}\right)^2\right] + \frac{1 - \frac{A_{rf}}{A_r}}{3}\left[\left(\frac{\bar{y}_r}{h_r}\right)^3 + \left(1 - \frac{\bar{y}_r}{h_r}\right)^3\right]$$

$$\frac{E_s A_s}{dE_x} = \frac{\frac{b_w}{d}\frac{t_w}{t_s}\left(1 + \frac{2\frac{b_f}{b_w}}{t_w/t_f}\right)}{E_o/E_s}$$

$$\frac{G_s J_s}{dD_x} = 0$$

$$\epsilon_s = \frac{E_s A_s/dE_x}{\frac{1}{1 - \mu^2} + \frac{E_r A_r}{\ell E_x}}\left(\pm \frac{\frac{\bar{Z}_s/h_s}{\sqrt{d_x/e_y}}}{h_s}\right)$$

where + and - indicate external and internal Z-stiffeners, respectively, and

$$\frac{\sqrt{d_x/e_y}}{h_s} = \frac{1}{b_w/d}\sqrt{\frac{\frac{t_w}{t_s}\left(\frac{b_w}{d}\right)^3\left(\frac{1}{6} + \frac{b_f/b_w}{t_w/t_f}\right)}{2\frac{E_o}{E_s}\left(\frac{1}{1 - \mu^2} + \frac{E_r A_r}{\ell E_x}\right)}}$$

$$\frac{\bar{Z}_s}{h_s} = \frac{\bar{y}_s}{b_w} = \frac{1}{2}$$

$$\frac{E_x}{e_x} = \frac{1}{\frac{1}{1 - \mu^2} + \frac{E_s A_s}{d E_x}}$$

$$\frac{E_x}{e_y} = \frac{1}{\frac{1}{1 - \mu^2} + \frac{E_r A_r}{\ell E_x}}$$

$$\frac{D_x}{d_x} = 0$$

$$\alpha = 1$$

$$K_1 = \frac{1}{\frac{1}{1 - \mu^2} + \frac{E_s A_s}{d E_x}}$$

$$K_2 = \frac{K_b \pi^2}{12\left(1 - \mu^2\right)}$$

$$\frac{A_r}{h_r t_{rw}} = \frac{1}{1 - \frac{A_{rf}}{A_r}}$$

$$\lambda = \frac{\frac{E_s}{E_o} \frac{t_w}{t_s} \left(\frac{b_w}{d}\right)^3 \left(\frac{1}{6} + \frac{b_f/b_w}{t_w/t_f}\right)}{2\left(\frac{1}{1 - \mu^2} + \frac{E_s A_s}{d E_x}\right)}$$

$$V_1 = \frac{E_r A_r / \ell E_x}{\frac{1}{1 - \mu^2} + \frac{E_r A_r}{\ell E_x}}$$

$$V_2 = 0$$

$$V_3 = \frac{2 \frac{E_r A_r}{\ell E_x} \frac{E_o}{E_s} \frac{I_r}{A_r h_r^2} \left(\frac{h_r}{d}\right)^2}{\frac{t_w}{t_s} \left(\frac{b_w}{d}\right)^3 \left(\frac{1}{6} + \frac{b_f/b_w}{t_w/t_f}\right)}$$

Dimensions (normalized by the cylinder radius R) and the local stress can be expressed as a function of the structural index N_x/E_oR as

$$\frac{t_s}{R} = \frac{\left(\frac{N_x}{E_oR}\right)^{3/5}}{\left(1 + \frac{E_rA_r}{\ell E_x}\frac{E_o}{E_r}\frac{\gamma_r}{\gamma_o} + \frac{E_sA_s}{dE_x}\frac{E_o}{E_s}\frac{\gamma_s}{\gamma_o}\right)F_s}$$

$$\frac{d}{R} = \frac{K_2{}^{1/2}\left(1 + \frac{E_sA_s}{dE_x}\frac{E_o}{E_s}\frac{\gamma_s}{\gamma_o}\right)^{1/2}\left(\frac{N_x}{E_oR}\right)^{2/5}}{\left(1 + \frac{E_rA_r}{\ell E_x}\frac{E_o}{E_r}\frac{\gamma_r}{\gamma_o} + \frac{E_sA_s}{dE_x}\frac{E_o}{E_s}\frac{\gamma_s}{\gamma_o}\right)^{3/2}F_s{}^{3/2}}$$

$$\frac{h_r}{R} = \frac{\frac{h_r}{d}K_2{}^{1/2}\left(1 + \frac{E_sA_s}{dE_x}\frac{E_o}{E_s}\frac{\gamma_s}{\gamma_o}\right)^{1/2}\left(\frac{N_x}{E_oR}\right)^{2/5}}{\left(1 + \frac{E_rA_r}{\ell E_x}\frac{E_o}{E_r}\frac{\gamma_r}{\gamma_o} + \frac{E_sA_s}{dE_x}\frac{E_o}{E_s}\frac{\gamma_s}{\gamma_o}\right)^{3/2}F_s{}^{3/2}}$$

$$\frac{\ell}{R} = \frac{K_2\left(\frac{A_r}{h_rt_{rw}}\right)\left(\frac{h_r}{d}\right)^2\left(1 + \frac{E_sA_s}{dE_x}\frac{E_o}{E_s}\frac{\gamma_s}{\gamma_o}\right)\left(\frac{N_x}{E_oR}\right)^{1/5}}{\left(1 + \frac{E_rA_r}{\ell E_x}\frac{E_o}{E_r}\frac{\gamma_r}{\gamma_o} + \frac{E_sA_s}{dE_x}\frac{E_o}{E_s}\frac{\gamma_s}{\gamma_o}\right)^2\frac{E_rA_r}{\ell E_x}\frac{E_o}{E_r}\frac{h_r}{t_{rw}}F_s{}^2}$$

$$\frac{A_r}{R^2} = \frac{K_2\left(\frac{A_r}{h_rt_{rw}}\right)\left(\frac{h_r}{d}\right)^2\left(1 + \frac{E_sA_s}{dE_x}\frac{E_o}{E_s}\frac{\gamma_s}{\gamma_o}\right)\left(\frac{N_x}{E_oR}\right)^{4/5}}{\left(1 + \frac{E_rA_r}{\ell E_x}\frac{E_o}{E_r}\frac{\gamma_r}{\gamma_o} + \frac{E_sA_s}{dE_x}\frac{E_o}{E_s}\frac{\gamma_s}{\gamma_o}\right)^3\left(\frac{h_r}{t_{rw}}\right)F_s{}^3}$$

$$\frac{\sigma_{cr}}{E_o} = \frac{\left(1 + \frac{E_rA_r}{\ell E_x}\frac{E_o}{E_r}\frac{\gamma_r}{\gamma_o} + \frac{E_sA_s}{dE_x}\frac{E_o}{E_s}\frac{\gamma_s}{\gamma_o}\right)F_s\left(\frac{N_x}{E_oR}\right)^{2/5}}{1 + \frac{E_sA_s}{dE_x}\frac{E_o}{E_s}\frac{\gamma_s}{\gamma_o}}$$

APPENDIX D

DOUBLE BEAD

This appendix contains the general terms needed for the mass-strength analysis of a ring-stiffened double-beaded cylinder. Also included are the geometric parameters used to describe the wall configuration and the optimum dimensions of the configuration expressed as a function of the structural index N_x/E_oR.

The geometry of the double bead is illustrated in figure 2(c). The dimension and thickness of the characteristic element is b and t_b. The parameters used to describe this configuration are as follows:

Design variables

$$\frac{\theta_a}{\theta_b} = 1, \frac{1}{3}$$

$$\theta_b = \pi$$

$$\frac{b}{P} = 0.4$$

Other parameters

$n = 1.35$ (Empirical value taken from ref. 5)

$\mu = 0.32$

$\frac{t_a}{t_b} = \frac{a}{b}$ (Constraint for equal local buckling)

$$\frac{a}{b} = \frac{\sin\frac{\theta_b}{2}}{\sin\left(\frac{\theta_a}{\theta_b}\frac{\theta_b}{2}\right)}$$

Expressions for the stiffnesses of the double bead are

$$E_x = E_o t_b \frac{b}{P} \Delta_3$$

$$E_y = D_y = 0$$

$$D_x = E_o b^2 t_b \frac{b}{P}\left(\Delta_1 - \frac{\Delta_2^2}{\Delta_3}\right)$$

$$D_{xy} = \frac{E_o \frac{b}{P} b^2 t_b \Delta_4^2}{4\theta_b(1+\mu)\left(\frac{\theta_a}{\theta_b}+1\right)}$$

$$G_{xy} = \frac{E_o t_b}{2(1+\mu)}\left(\frac{\sin\frac{\theta_b}{2}}{\left\{1+\frac{b}{P}\left[\frac{\theta_b\frac{\theta_a}{\theta_b}\sin\frac{\theta_b}{2}}{\sin\left(\frac{\theta_a}{\theta_b}\frac{\theta_b}{2}\right)}-2\right]\right\}\left[\sin\left(\frac{\theta_a}{\theta_b}\frac{\theta_b}{2}\right)\right]}+\frac{1}{1+\frac{b}{P}(\theta_b-2)}\right)$$

$$\mu_x = \mu_y = \mu'_x = \mu'_y = 0$$

where

$$\Delta_1 = \frac{\theta_b}{2}+\frac{\sin\frac{\theta_b}{2}}{\sin\left(\frac{\theta_a}{\theta_b}\frac{\theta_b}{2}\right)}\left\{\frac{3}{2}-\left[\frac{\sin\left(\frac{\theta_a}{\theta_b}\frac{\theta_b}{2}\right)}{\sin\frac{\theta_b}{2}}\right]^2\theta_b\frac{\theta_a}{\theta_b}-\frac{3\sin\left(\frac{\theta_a}{\theta_b}\frac{\theta_b}{2}\right)\cos\left(\frac{\theta_a}{\theta_b}\frac{\theta_b}{2}\right)}{\sin\frac{\theta_b}{2}}\right\}$$

$$\Delta_2 = 2-2\left[\frac{\sin\frac{\theta_b}{2}}{\sin\left(\frac{\theta_a}{\theta_b}\frac{\theta_b}{2}\right)}\right]^3\left[\frac{\sin\left(\frac{\theta_a}{\theta_b}\frac{\theta_b}{2}\right)}{\sin\frac{\theta_b}{2}}-\frac{\theta_a}{\theta_b}\frac{\theta_b}{2}\cos\left(\frac{\theta_a}{\theta_b}\frac{\theta_b}{2}\right)\right]$$

$$\Delta_3 = \theta_b+\left[\frac{\sin\frac{\theta_b}{2}}{\sin\left(\frac{\theta_a}{\theta_b}\frac{\theta_b}{2}\right)}\right]^2\frac{\theta_a}{\theta_b}\theta_b+\left(\frac{1}{b/P}-2\right)\left[\frac{\sin\frac{\theta_b}{2}}{\sin\left(\frac{\theta_a}{\theta_b}\frac{\theta_b}{2}\right)}+1\right]$$

$$\Delta_4 = \theta_b+\left[\frac{\sin\frac{\theta_b}{2}}{\sin\left(\frac{\theta_a}{\theta_b}\frac{\theta_b}{2}\right)}\right]^2\frac{\theta_a}{\theta_b}\theta_b-\frac{\sin^2\frac{\theta_b}{2}\sin\left(\frac{\theta_a}{\theta_b}\theta_b\right)}{\sin^2\left(\frac{\theta_a}{\theta_b}\frac{\theta_b}{2}\right)}$$

The expressions used in the mass-strength analysis are

$$\frac{e_x}{e_y} = \frac{1}{E_r A_r/\ell E_x}$$

$$g_{xy} = \frac{\sin\frac{\theta_b}{2}\left[1 + \frac{b}{P}(\theta_b - 2)\right] + \left\{1 + \frac{b}{P}\left[\frac{\sin\frac{\theta_b}{2}}{\sin\left(\frac{\theta_a}{\theta_b}\frac{\theta_b}{2}\right)}\frac{\theta_a}{\theta_b}\theta_b - 2\right]\right\}}{2(1+\mu)\left(\frac{b}{P}\right)\Delta_3\frac{E_r A_r}{\ell E_x}\left[1 + \frac{b}{P}(\theta_b - 2)\right]\left\{1 + \frac{b}{P}\left[\frac{\sin\frac{\theta_b}{2}}{\sin\left(\frac{\theta_a}{\theta_b}\frac{\theta_b}{2}\right)}\frac{\theta_a}{\theta_b}\theta_b - 2\right]\right\}\sin\left(\frac{\theta_a}{\theta_b}\frac{\theta_b}{2}\right)}$$

$i = 0$

$$\epsilon_{r(\text{tubular})} = \pm\frac{\frac{\bar{y}_r}{h_r} \pm \frac{\bar{y}}{h_r}}{\frac{\sqrt{d_x/e_y}}{h_r}}$$

$$\epsilon_{r(\text{nonsymmetric, internal rings})} = -\frac{\frac{\bar{y}_r}{h_r} - \frac{\bar{y}}{h_r} + \frac{1}{h_r/b}}{\frac{\sqrt{d_x/e_y}}{h_r}}$$

where + and - indicate external and internal rings, respectively, and

$$\frac{\bar{y}_r}{h_r} = (1 - k_r)\frac{A_{rf}}{A_r} + \frac{1}{2\frac{A_r}{h_r t_{rw}}}$$

$$\frac{\sqrt{d_x/e_y}}{h_r} = \frac{1}{h_r/b}\sqrt{\frac{\Delta_1 - \frac{\Delta_2^2}{\Delta_3}}{\Delta_3\frac{E_r A_r}{\ell E_x}}}$$

$$\frac{\bar{y}}{h_r} = \frac{\Delta_2}{\frac{h_r}{b}\Delta_3}$$

$$\frac{d_{xy}}{d_x} = \frac{G_r J_r}{\ell D_x} + \frac{\Delta_4^2}{2(1+\mu)\theta_b\left(\frac{\theta_a}{\theta_b}+1\right)\left(\Delta_1 - \frac{\Delta_2^2}{\Delta_3}\right)}$$

$$\frac{d_y}{d_x} = \frac{E_r I_r}{\ell D_x} = \left(\frac{h_r}{b}\right)^2 \frac{E_r A_r}{\ell D_x} \frac{\Delta_3}{\Delta_1 - \frac{\Delta_2^2}{\Delta_3}} \left\{ \frac{A_{rf}}{A_r}\left[(1-k_r)\left(1-\frac{\bar{y}_r}{h_r}\right)^2 + k_r\left(\frac{\bar{y}_r}{h_r}\right)^2\right] + \frac{\left(\frac{\bar{y}_r}{h_r}\right)^3 + \left(1-\frac{\bar{y}_r}{h_r}\right)^3}{3\frac{A_r}{h_r t_{rw}}} \right\}$$

$$\frac{E_x}{e_y} = \frac{1}{E_r A_r / \ell E_x}$$

$$\frac{D_x}{d_x} = \alpha = \frac{E_x}{e_x} = 1$$

$$K_1 = \frac{1}{\frac{b}{P}\Delta_3}$$

$K_2 = 1.75$ (Empirical value taken from ref. 5, good for $50 < \frac{b}{t_b} < 500$)

$$\frac{A_r}{h_r t_{rw}} = \frac{1}{1 - \frac{A_{rf}}{A_r}}$$

$$\lambda = \frac{\Delta_1 - \frac{\Delta_2^2}{\Delta_3}}{\Delta_3}$$

$$V_1 = 1$$

$$V_2 = \frac{G_r J_r}{\ell E_x}$$

$$V_3 = \frac{E_r I_r}{\ell D_x}$$

The dimensions (normalized by the cylinder radius R) and the local stress can be expressed as a function of the structural index N_x/E_oR as

$$\frac{t_b}{R} = \frac{\left(\frac{N_x}{E_oR}\right)^{0.635}}{\frac{b}{P}\Delta_3 F_s\left(\alpha + \frac{E_rA_r}{\ell E_x}\frac{E_o}{E_r}\frac{\gamma_r}{\gamma_o}\right)}$$

$$\frac{b}{R} = \frac{K_2^{0.74}}{\frac{b}{P}\Delta_3\left[\left(\alpha + \frac{E_rA_r}{\ell E_x}\frac{E_o}{E_r}\frac{\gamma_r}{\gamma_o}\right)F_s\right]^{1.74}}\left(\frac{N_x}{E_oR}\right)^{0.365}$$

$$\frac{h_r}{R} = \frac{\frac{h_r}{b}K_2^{0.74}}{\frac{b}{P}\Delta_3\left[\left(\alpha + \frac{E_rA_r}{\ell E_x}\frac{E_o}{E_r}\frac{\gamma_r}{\gamma_o}\right)F_s\right]^{1.74}}\left(\frac{N_x}{E_oR}\right)^{0.365}$$

$$\frac{\ell}{R} = \frac{\frac{A_r}{h_rt_{rw}}\left(\frac{h_r}{b}\right)^2 K_2^{1.48}}{\frac{E_o}{E_r}\frac{h_r}{t_{rw}}\left(\frac{b}{P}\right)^2\Delta_3^2\frac{E_rA_r}{\ell E_x}\left[\left(\alpha + \frac{E_rA_r}{\ell E_x}\frac{E_o}{E_r}\frac{\gamma_r}{\gamma_o}\right)F_s\right]^{2.48}}\left(\frac{N_x}{E_oR}\right)^{0.095}$$

$$\frac{A_r}{R^2} = \frac{\frac{A_r}{h_rt_{rw}}K_2^{1.48}\left(\frac{h_r}{b}\right)^2}{\frac{h_r}{t_{rw}}\left(\frac{b}{P}\right)^2\Delta_3^2\left[\left(\alpha + \frac{E_rA_r}{\ell E_x}\frac{E_o}{E_r}\frac{\gamma_r}{\gamma_o}\right)F_s\right]^{3.48}}\left(\frac{N_x}{E_oR}\right)^{0.73}$$

$$\frac{\sigma_{cr}}{E_o} = \left(\alpha + \frac{E_rA_r}{\ell E_x}\frac{E_o}{E_r}\frac{\gamma_r}{\gamma_o}\right)F_s\left(\frac{N_x}{E_oR}\right)^{0.365}$$

REFERENCES

1. Gerard, George: Optimum Structural Design Concepts for Aerospace Vehicles. J. Spacecraft, vol. 3, no. 1, Jan. 1966, pp. 5-18.

2. Lakshmikantham, C.; and Becker, H.: Minimum Weight Design Aspects of Stiffened Cylinders Under Compression. NASA CR-963, 1967.

3. Peterson, James P.: Structural Efficiency of Ring-Stiffened Corrugated Cylinders in Axial Compression. NASA TN D-4073, 1967.

4. Singer, Josef; and Baruch, Menahem: Recent Studies on Optimisation for Elastic Stability of Cylindrical and Conical Shells. Aerospace Proceedings 1966, Vol. 2, Joan Bradbrooke, Joan Bruce, and Robert R. Dexter, eds., Macmillan and Co., Ltd., c.1967, pp. 751-782.

5. Giles, G. L.: Structural Efficiencies of Five Compression Panels With Curved Elements. NASA TN D-6479, 1971.

6. Block, David L.; Card, Michael F.; and Mikulas, Martin M., Jr.: Buckling of Eccentrically Stiffened Orthotropic Cylinders. NASA TN D-2960, 1965.

7. Stowell, Elbridge Z.; Heimerl, George J.; Libove, Charles; and Lundquist, Eugene E.: Buckling Stresses for Flat Plates and Sections. Paper No. 2506, Trans. American Soc. Civil Eng., vol. 117, 1952, pp. 545-575; Discussion, pp. 576-578.

8. Gallaher, George L.; and Boughan, Rolla B.: A Method of Calculating the Compressive Strength of Z-Stiffened Panels That Develop Local Instability. NACA TN 1482, 1947.

9. Peterson, James P.: Weight-Strength Studies of Structures Representative of Fuselage Construction. NACA TN 4114, 1957.

10. Gerard, George; and Papirno, Ralph: Minimum Weight Design of Stiffened Cylinders for Launch Vehicle Applications. Tech. Rep. No. 235-5, Allied Res. Assoc., Inc., Mar. 13, 1964. (Available as NASA CR-53317.)

11. Anderson, Melvin S.; and Stroud, C. W.: Experimental Observations of Aerodynamic and Heating Tests on Insulating Heat Shields. NASA TN D-1237, 1962.

12. Seide, P.; Weingarten, V. I.; and Morgan, E. J.: Final Report on the Development of Design Criteria for Elastic Stability of Thin Shell Structures. AFBMD/TR-61-7, U.S. Air Force, Dec. 31, 1960.

13. Emero, Donald H.; and Spunt, Leonard: Optimization of Multirib and Multiweb Wing Box Structures Under Shear and Moment Loads. AIAA 6th Structures and Material Conference, Apr. 1965, pp. 330-353.

14. Comm. on Metric Pract.: ASTM Metric Practice Guide. NBS Handbook 102, U.S. Dep. Com., Mar. 10, 1967.

15. Jackson, L. Robert; Davis, John G., Jr.; and Wichorek, Gregory R.: Structural Concepts for Hydrogen-Fueled Hypersonic Airplanes. NASA TN D-3162, 1966.

TABLE I.- RESULTS

(a) Trapezoidal corrugation; n = 2

$\frac{\bar{t}}{R}$	$\frac{N_x}{E_o R}$	φ_{opt}	n_g	$\beta^2_{g,opt}$	$\beta^2_{p,opt}$	$\frac{h_r}{b}$	$F_{s,opt}$	$\frac{t_b}{R}$	$\frac{\sigma_{cr}}{E_o}$	$\frac{b}{R}$	$\frac{h_r}{R}$	$\frac{\ell}{R}$	$\frac{A_r}{R^2}$	Design variables			Other parameters	Ring parameters		
														$\frac{a}{b}$	θ, deg	$\frac{t_a}{t_b}$	K_b	$\frac{E_r A_r}{\ell E_x}$	$\frac{A_{rf}}{A_r}$	k_r (a)
Internal rings																				
1.0×10^{-4}	6.39×10^{-8}	1.11	8.1	0.523	0	2.47	0.483	5.82×10^{-5}	8.44×10^{-4}	4.02×10^{-3}	9.93×10^{-3}	1.45×10^{-1}	3.52×10^{-6}	0.90	56	1.0	4.4	0.32	0.65	0.8
7.0×10^{-4}	1.64×10^{-6}	1.11	4.2	.523	0	2.47	.483	4.07×10^{-4}	3.09×10^{-3}	1.47×10^{-2}	3.63×10^{-2}	2.78×10^{-1}	4.71×10^{-5}	.90	56	1.0	4.4	.32	.65	.8
1.7×10^{-3}	6.95×10^{-6}	1.06	3.1	.802	0	2.12	.474	1.10×10^{-3}	4.91×10^{-3}	3.07×10^{-2}	6.48×10^{-2}	4.63×10^{-1}	1.31×10^{-4}	.95	56	1.0	4.2	.2	.60	.8
External rings																				
1.0×10^{-4}	9.56×10^{-8}	2.0	0	0	0	[b]2.23	0.613	6.02×10^{-5}	1.19×10^{-3}	3.50×10^{-3}	[b]7.80 $\times 10^{-3}$	1.09×10^{-1}	2.17×10^{-6}	0.90	58	1.0	4.4	0.25	[b]0.65	[b]0.8
7.0×10^{-4}	2.45×10^{-6}	2.0	0	0	0	[b]2.23	.613	4.21×10^{-4}	4.37×10^{-3}	1.28×10^{-2}	[b]2.85 $\times 10^{-2}$	2.08×10^{-1}	2.91×10^{-5}	.90	58	1.0	4.4	.25	[b].65	[b].8
1.2×10^{-3}	5.48×10^{-6}	2.0	0	0	0	[b]1.41	.581	8.21×10^{-4}	5.02×10^{-3}	2.33×10^{-2}	[b]3.28 $\times 10^{-2}$	3.52×10^{-1}	3.84×10^{-5}	.90	58	1.0	4.4	.10	[b].65	[b].8

[a] Limited to values between 0.2 and 0.8.

[b] Optimum solution is independent of ring shape for external rings (positive eccentricity) if $\frac{E_r I_r}{\ell D_x} > \frac{E_r A_r}{\ell E_x}$ for $E_y = 0$ (see ref. 3). These values of the ring parameters satisfy this inequality and are therefore not unique to the optimum solution.

TABLE I.- RESULTS – Continued

(b) Z-stiffened skin; n = 2; $\frac{b_f}{b_w} = 0.4$

$\frac{\bar{t}}{R}$	$\frac{N_x}{E_o R}$	φ_{opt}	n_g	$\beta^2_{g,opt}$	$\beta^2_{p,opt}$	$\frac{h_r}{d}$	$F_{s,opt}$	$\frac{t_s}{R}$	$\frac{\sigma_{cr}}{E_o}$	$\frac{d}{R}$	$\frac{h_r}{R}$	$\frac{\ell}{R}$	$\frac{A_r}{R^2}$	Design variables			Other parameters	Ring parameters		
														$\frac{b_w}{d}$	$\frac{t_w}{t_s}$	$\frac{t_w}{t_f}$	K_b	$\frac{E_r A_r}{\ell E_x}$	$\frac{A_{rf}}{A_r}$	k_r (a)
Internal Z-stiffeners; internal rings																				
1.0×10^{-4}	8.87×10^{-8}	2.09	21.6	0.346	1.61	2.20	0.587	5.22×10^{-5}	9.68×10^{-4}	2.98×10^{-3}	6.56×10^{-3}	7.59×10^{-2}	6.34×10^{-7}	0.70	0.60	1.0	3.45	0.16	0.15	0.2
8.0×10^{-4}	2.84×10^{-6}	2.09	10.8	.346	1.61	2.20	.587	4.18×10^{-4}	3.87×10^{-3}	1.19×10^{-2}	2.62×10^{-2}	1.52×10^{-1}	1.01×10^{-5}	.70	.60	1.0	3.45	.16	.15	.2
1.25×10^{-3}	5.89×10^{-6}	2.04	11.6	.469	1.77	1.54	.582	7.38×10^{-4}	5.01×10^{-3}	1.93×10^{-2}	2.97×10^{-2}	1.76×10^{-1}	1.30×10^{-5}	.60	.55	1.0	3.75	.10	.15	.2
Internal Z-stiffeners; external rings																				
1.0×10^{-4}	9.97×10^{-8}	2.82	19.5	0.163	1.23	3.01	0.630	4.86×10^{-5}	1.17×10^{-3}	2.53×10^{-3}	7.62×10^{-3}	5.85×10^{-2}	8.54×10^{-7}	0.70	0.60	1.0	3.45	0.30	0.15	0.2
8.0×10^{-4}	3.19×10^{-6}	2.82	9.7	.163	1.23	3.01	.630	3.89×10^{-4}	4.67×10^{-3}	1.01×10^{-2}	3.05×10^{-2}	1.17×10^{-1}	1.37×10^{-5}	.70	.60	1.0	3.45	.30	.15	.2
1.3×10^{-3}	6.07×10^{-6}	2.16	15.9	.699	1.83	1.33	.570	8.39×10^{-4}	4.99×10^{-3}	2.29×10^{-2}	3.05×10^{-2}	1.63×10^{-1}	1.36×10^{-5}	.50	.50	1.0	4.05	.10	.15	.2
Internal Z-stiffeners; internal rings at skin																				
1.0×10^{-4}	8.32×10^{-8}	2.00	22.4	0.379	1.64	2.58	0.565	5.06×10^{-5}	9.36×10^{-4}	2.94×10^{-3}	7.58×10^{-1}	7.59×10^{-2}	8.45×10^{-7}	0.70	0.60	1.0	3.45	0.22	0.15	0.2
8.0×10^{-4}	2.66×10^{-6}	2.00	11.2	.379	1.64	2.58	.565	4.05×10^{-4}	3.75×10^{-3}	1.18×10^{-2}	3.03×10^{-2}	1.52×10^{-1}	1.35×10^{-5}	.70	.60	1.0	3.45	.22	.15	.2
1.5×10^{-3}	7.09×10^{-6}	1.71	12.3	.829	2.07	1.54	.542	8.86×10^{-4}	5.02×10^{-3}	2.32×10^{-2}	3.56×10^{-2}	2.11×10^{-1}	1.87×10^{-5}	.60	.55	1.0	3.75	.10	.15	.2
External Z-stiffeners; internal rings																				
1.0×10^{-4}	8.56×10^{-8}	1.91	24.8	0.449	3.66	2.05	0.575	5.33×10^{-5}	9.15×10^{-4}	3.13×10^{-3}	6.41×10^{-3}	9.46×10^{-2}	6.05×10^{-7}	0.70	0.60	1.0	3.45	0.12	0.15	0.2
8.0×10^{-4}	2.74×10^{-6}	1.91	12.4	.449	3.66	2.05	.575	4.26×10^{-4}	3.66×10^{-3}	1.25×10^{-2}	2.57×10^{-2}	1.89×10^{-1}	9.68×10^{-6}	.70	.60	1.0	3.45	.12	.15	.2
1.3×10^{-3}	6.15×10^{-6}	1.87	11.3	.612	5.02	1.87	.575	7.00×10^{-4}	5.00×10^{-3}	1.76×10^{-2}	3.30×10^{-2}	2.28×10^{-1}	1.60×10^{-5}	.70	.60	1.0	3.45	.10	.15	.2
External Z-stiffeners; external rings																				
1.0×10^{-4}	9.92×10^{-8}	2.29	16.6	0.135	1.01	1.70	0.628	5.45×10^{-5}	1.04×10^{-3}	3.01×10^{-3}	5.10×10^{-3}	8.30×10^{-2}	3.62×10^{-7}	0.70	0.60	1.0	3.45	0.08	0.10	0.2
8.0×10^{-4}	3.17×10^{-6}	2.29	8.3	.135	1.01	1.70	.628	4.36×10^{-4}	4.15×10^{-3}	1.20×10^{-2}	2.04×10^{-2}	1.66×10^{-1}	5.78×10^{-6}	.70	.60	1.0	3.45	.08	.10	.2
External Z-stiffeners; external rings at skin																				
1.0×10^{-4}	9.64×10^{-8}	2.28	19.4	0.192	0.874	2.02	0.617	5.33×10^{-5}	1.03×10^{-3}	2.95×10^{-3}	5.96×10^{-3}	8.15×10^{-2}	5.21×10^{-7}	0.70	0.60	1.0	3.45	0.12	0.15	0.2
8.0×10^{-4}	3.09×10^{-6}	2.28	9.7	.192	.874	2.02	.617	4.26×10^{-4}	4.12×10^{-3}	1.18×10^{-2}	2.38×10^{-2}	1.63×10^{-1}	8.34×10^{-6}	.70	.60	1.0	3.45	.12	.15	.2
1.1×10^{-3}	5.20×10^{-6}	2.22	10.8	.367	1.22	1.85	.615	5.93×10^{-4}	5.00×10^{-3}	1.49×10^{-2}	2.75×10^{-2}	1.88×10^{-1}	1.11×10^{-5}	.70	.60	1.0	3.45	.10	.15	.2

[a] Limited to values between 0.2 and 0.8.

TABLE I.- RESULTS – Concluded

(c) Double bead, n = 1.35

$\frac{\bar{t}}{R}$	$\frac{N_x}{E_o R}$	φ_{opt}	n_g	$\beta^2_{g,opt}$	$\beta^2_{p,opt}$	$\frac{h_r}{b}$	$F_{s,opt}$	$\frac{t_b}{R}$	$\frac{\sigma_{cr}}{E_o}$	$\frac{b}{R}$	$\frac{h_r}{R}$	$\frac{\ell}{R}$	$\frac{A_r}{R^2}$	Design variables			Other parameters		Ring parameters		
														θ_b, deg	$\frac{\theta_a}{\theta_b}$	$\frac{b}{P}$	K_2	$\frac{a}{b}$	$\frac{E_r A_r}{\ell E_x}$	$\frac{A_{rf}}{A_r}$	k_r (a)
Tubular; internal rings																					
1.0×10^{-4}	1.68×10^{-7}	1.71	8.0	3.53	0	1.59	0.500	3.06×10^{-5}	1.88×10^{-3}	4.81×10^{-3}	7.65×10^{-3}	2.28×10^{-1}	2.44×10^{-6}	180	1.0	0.4	1.75	1.0	0.12	0.70	0.8
3.0×10^{-4}	9.54×10^{-7}	1.73	5.8	2.59	0	1.72	.503	9.19×10^{-5}	3.56×10^{-3}	9.02×10^{-3}	1.55×10^{-2}	3.11×10^{-1}	9.99×10^{-6}	180	1.0	.4	1.75	1.0	.12	.70	.8
5.6×10^{-4}	2.55×10^{-6}	1.80	4.8	3.53	0	1.63	.503	1.75×10^{-4}	5.01×10^{-3}	1.33×10^{-2}	2.17×10^{-2}	3.87×10^{-1}	1.97×10^{-5}	180	1.0	.4	1.75	1.0	.10	.70	.8
Tubular; external rings																					
1.0×10^{-4}	1.91×10^{-7}	2.0	0	0	0	[b]2.21	0.542	2.81×10^{-5}	2.34×10^{-3}	3.77×10^{-3}	[b]8.33×10^{-3}	1.60×10^{-1}	2.89×10^{-6}	180	1.0	0.4	1.75	1.0	0.22	[b]0.70	[b]0.8
3.0×10^{-4}	1.08×10^{-6}	2.0	0	0	0	[b]2.38	.542	8.44×10^{-5}	4.39×10^{-3}	7.09×10^{-3}	[b]1.69×10^{-2}	2.20×10^{-1}	1.19×10^{-5}	180	1.0	.4	1.75	1.0	.22	[b].70	[b].8
5.0×10^{-4}	2.26×10^{-6}	2.0	0	0	0	[b]1.88	.520	1.56×10^{-4}	4.98×10^{-3}	1.19×10^{-2}	[b]1.94×10^{-2}	3.48×10^{-1}	1.58×10^{-5}	180	1.0	.4	1.75	1.0	.10	[b].60	[b].8
Unsymmetrical double bead; internal rings																					
1.0×10^{-4}	9.78×10^{-8}	1.19	12.7	1.24	0	1.74	0.353	2.40×10^{-5}	1.15×10^{-3}	5.46×10^{-3}	9.44×10^{-3}	2.08×10^{-1}	3.18×10^{-6}	180	0.333	0.4	1.75	2.0	0.18	0.65	0.8
7.0×10^{-4}	2.13×10^{-6}	1.22	7.2	1.14	0	1.85	.357	1.68×10^{-4}	3.58×10^{-3}	1.64×10^{-2}	3.03×10^{-2}	3.59×10^{-1}	3.83×10^{-5}	180	.333	.4	1.75	2.0	.18	.70	.8
1.4×10^{-3}	6.25×10^{-6}	1.32	5.8	2.01	0	1.43	.354	3.60×10^{-4}	4.91×10^{-3}	2.79×10^{-2}	3.99×10^{-2}	5.21×10^{-1}	6.63×10^{-5}	180	.333	.4	1.75	2.0	.10	.70	.8

[a] Limited to values between 0.2 and 0.8.

[b] Optimum solution is independent of ring shape for external rings (positive eccentricity) if $\frac{E_r I_r}{\ell D_x} > \frac{E_r A_r}{\ell E_x}$ for $E_y = 0$ (see ref. 3). These values of the ring parameters satisfy this inequality and are therefore not unique to the optimum solution.

TABLE II.- MASS COMPARISON OF CONFIGURATIONS

[N_x = 350.2 kN/m^2 (2000 lbf/in.); E_o = 68.9 GN/m^2 (10 × 10^6 lbf/in^2); R = 304.8 cm (120 in.); γ_o = 2768 kg/m^3 (0.1 lbm/in^3)]

(a) Configuration comparison. $N_x/E_oR = 1.67 \times 10^{-6}$; internal rings

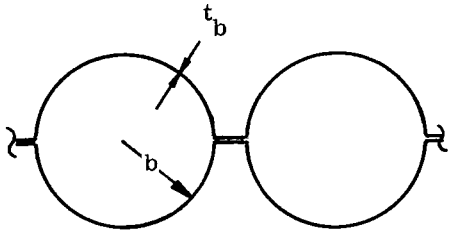

Tubular double bead

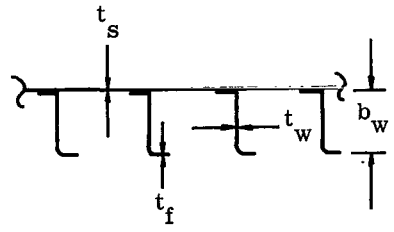

Z-stiffened

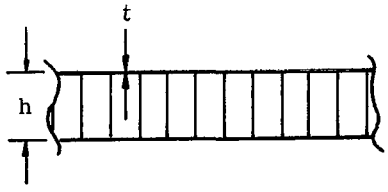

3-percent honeycomb sandwich

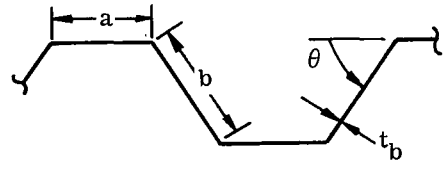

Trapezoidal corrugation

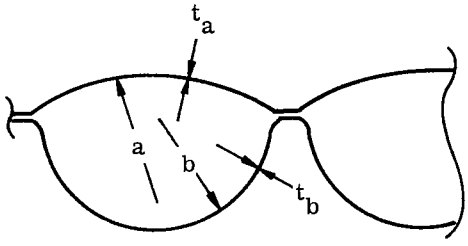

Nonsymmetric double bead

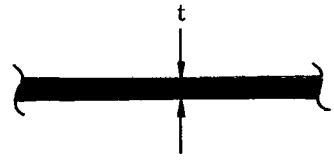

Unstiffened skin

TABLE II.- MASS COMPARISON OF CONFIGURATIONS – Concluded

(b) SI Units

Configuration	Internal rings						External rings					
	M_{shell}, kg/m^2	M_{ring}, kg/m^2	M_T, kg/m^2	Height, cm	Thickness, cm	Ring spacing, cm	M_{shell}, kg/m^2	M_{ring}, kg/m^2	M_T, kg/m^2	Height, cm	Thickness, cm	Ring spacing, cm
Tubular double bead	3.22	0.391	3.62	6.70	0.038	100.5	2.69	0.587	3.28	5.13	0.033	73.0
3-percent honeycomb sandwich; core depth, h	3.66	0	3.66	2.18	0.033	(a)						
Nonsymmetric double bead	4.20	0.780	4.98	[b] 5.82	0.043 .086	103.8						
Z-stiffened shell; external Z-stiffeners	[c] 2.69	0.342	5.08	2.18	0.096 .058	52.3	2.49	0.195	4.63	1.98	0.089 .053	47.0
Z-stiffened shell; internal Z-stiffeners	[c] 2.54	0.390	4.88	2.06	0.091 .056	42.4	2.20	0.683	4.63	1.68	0.081 .048	31.7
Z-stiffened shell; Z-stiffeners and rings attached to same side of shell	2.54	0.585	5.07	2.06	0.094 .056	42.7	2.49	0.293	4.73	1.98	0.089 .053	43.9
Trapezoidal corrugation	4.54	1.42	5.96	3.68	0.122	83.6	3.57	1.12	4.69	2.95	0.103	57.9
Unstiffened shell; thickness, t	22.0	0	22.0	0.790	0.792	(a)						

(c) U.S. Customary Units

Configuration	Internal rings						External rings					
	M_{shell}, lb/ft^2	M_{ring}, lb/ft^2	M_T, lb/ft^2	Height, in.	Thickness, in.	Ring spacing, in.	M_{shell}, lb/ft^2	M_{ring}, lb/ft^2	M_T, lb/ft^2	Height, in.	Thickness, in.	Ring spacing, in.
Tubular double bead	0.66	0.08	0.74	2b = 2.64	t_b = 0.015	39.6	0.55	0.12	0.67	2b = 2.02	t_b = 0.013	28.8
3-percent honeycomb sandwich; core depth, h	0.75	0	0.75	h = 0.86	t = 0.013	(a)						
Nonsymmetric double bead	0.86	0.16	1.02	[b] 2.29	t_b = 0.017 t_a = 0.034	40.8						
Z-stiffened shell; external Z-stiffeners	[c] 0.55	0.07	1.04	b_w = 0.86	t_s = 0.038 t_w = 0.023	20.6	0.51	0.04	0.95	b_w = 0.78	t_s = 0.035 t_w = 0.021	18.5
Z-stiffened shell; internal Z-stiffeners	[c] 0.52	0.08	1.00	b_w = 0.81	t_s = 0.036 t_w = 0.022	16.7	0.45	0.14	0.93	b_w = 0.66	t_s = 0.032 t_w = 0.019	12.5
Z-stiffened shell; Z-stiffeners and rings attached to same side of shell	[c] 0.52	0.12	1.04	b_w = 0.81	t_s = 0.037 t_w = 0.022	16.8	0.51	0.06	0.97	b_w = 0.78	t_s = 0.035 t_w = 0.021	17.3
Trapezoidal corrugation	0.93	0.29	1.22	b sin θ = 1.45	t_b = 0.048	33.0	0.73	0.23	0.96	b sin θ = 1.16	t_b = 0.040	22.8
Unstiffened shell; thickness, t	4.50	0	4.50	t = 0.312	t = 0.312	(a)						

[a] Does not have rings.

[b] Height = $b\left\{1 + \frac{a}{b} - \left[\left(\frac{a}{b}\right)^2 - 1\right]^{1/2}\right\}$.

[c] Mass of skin only.

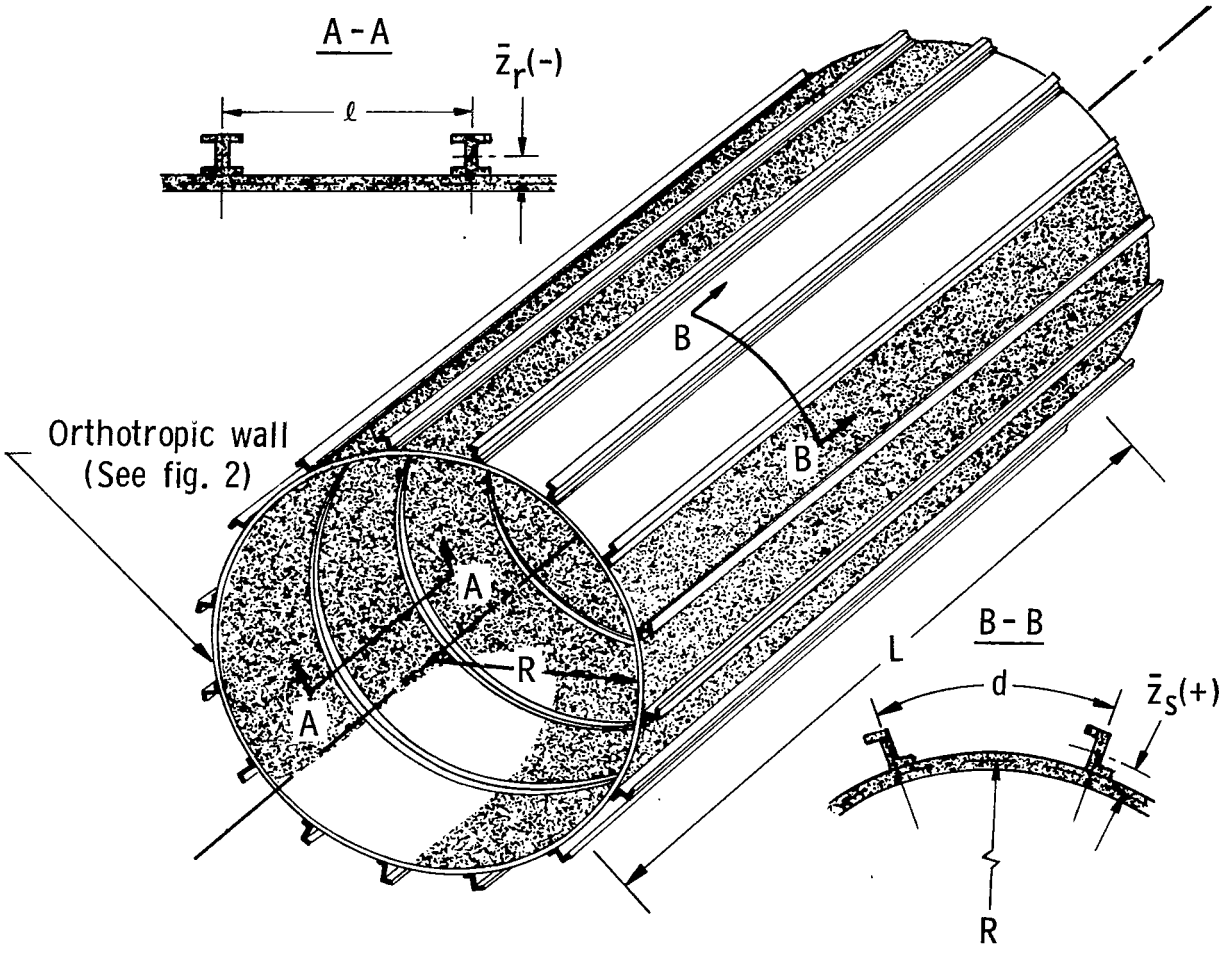

Figure 1.- Stiffened cylinder.

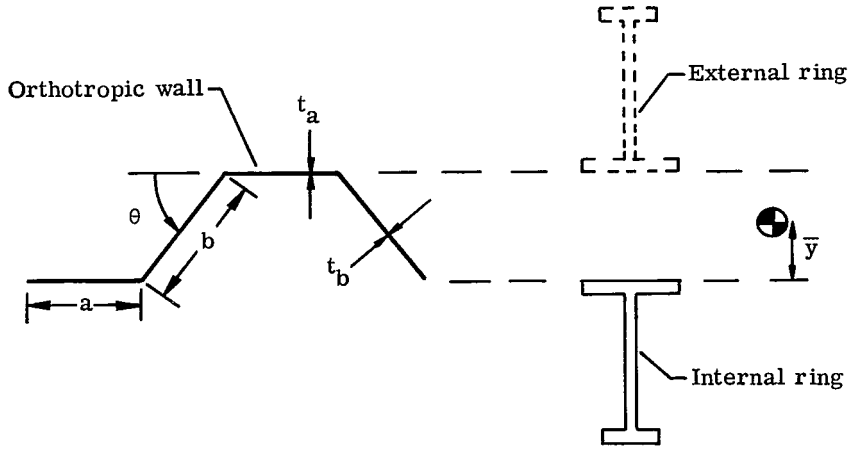

(a) Trapezoidal corrugation.

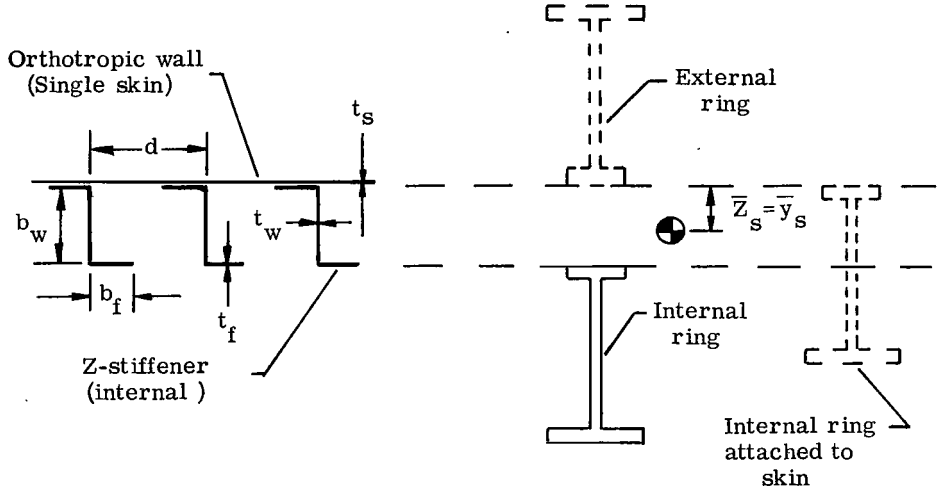

(b) Z-stiffened skin. (Internal rings are attached to skin; ring webs would have cutouts for Z-stiffeners.)

Figure 2.- Orthotropic wall and ring geometries.

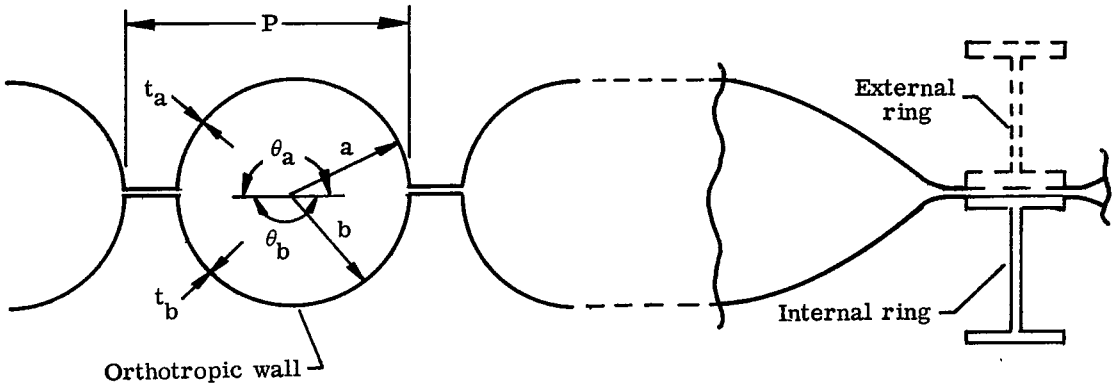

(c) Tubular double bead.

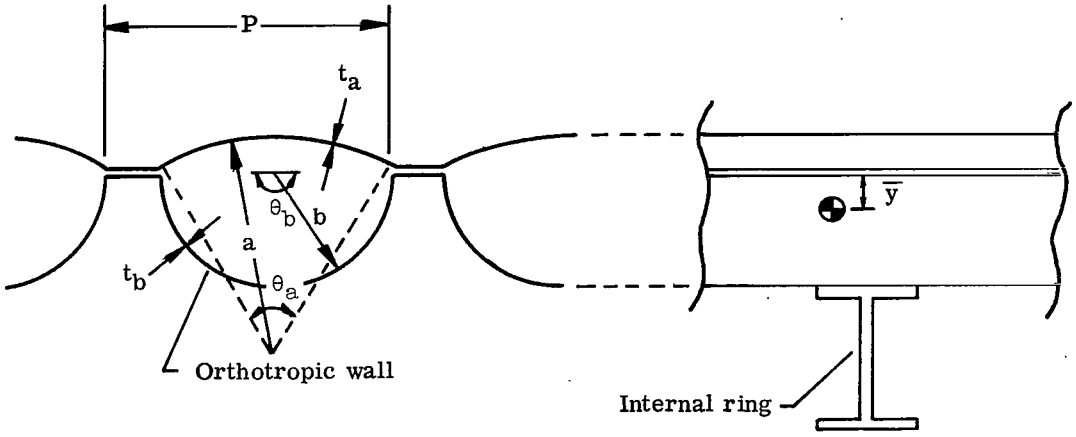

(d) Unsymmetric double bead. a/b = 2.

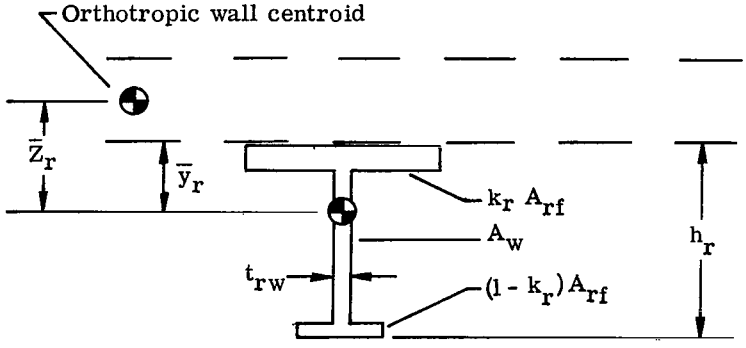

(e) Ring.

Figure 2.- Concluded.

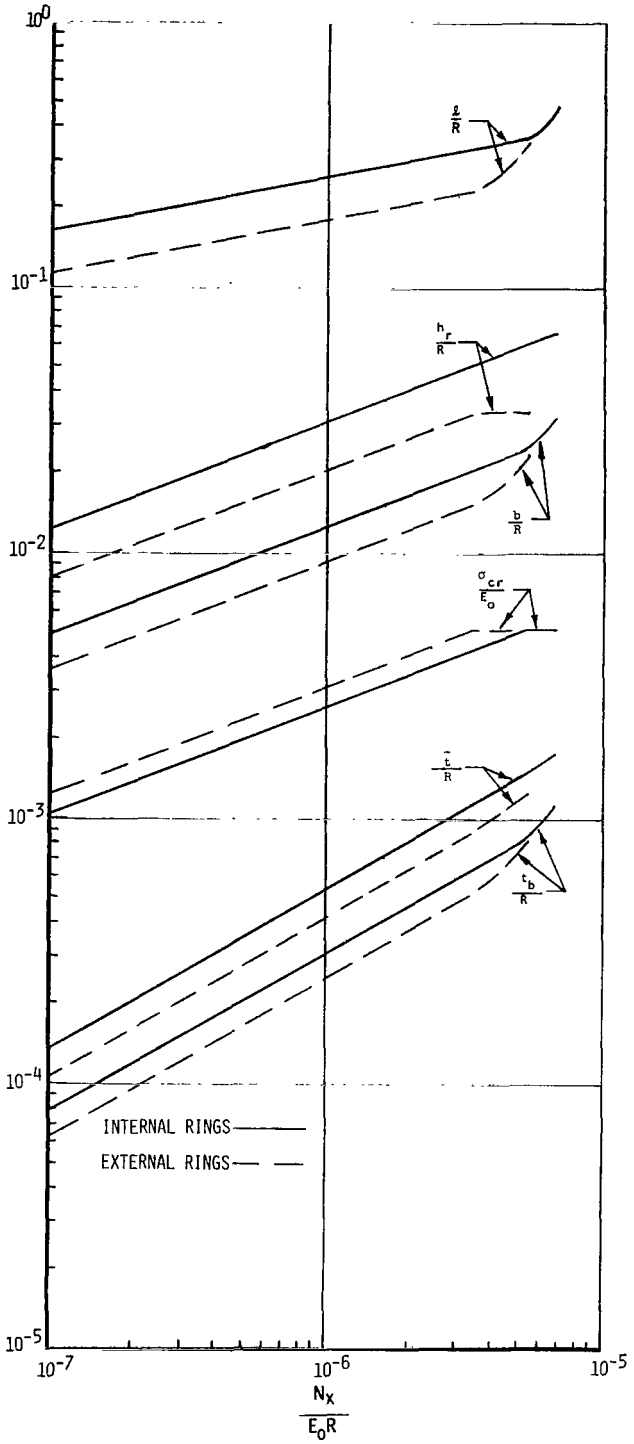

Figure 3.- Trapezoidal corrugation.

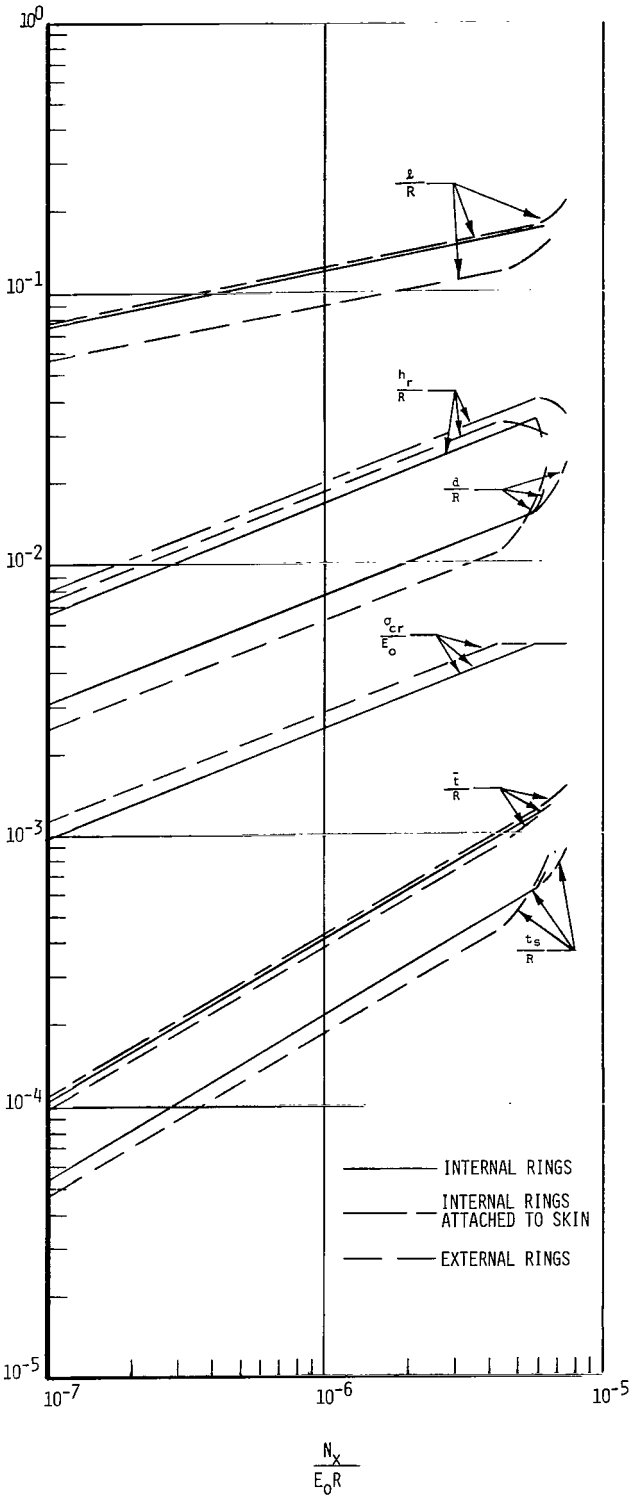

(a) Internal Z-stiffeners.

Figure 4.- Z-stiffened skin.

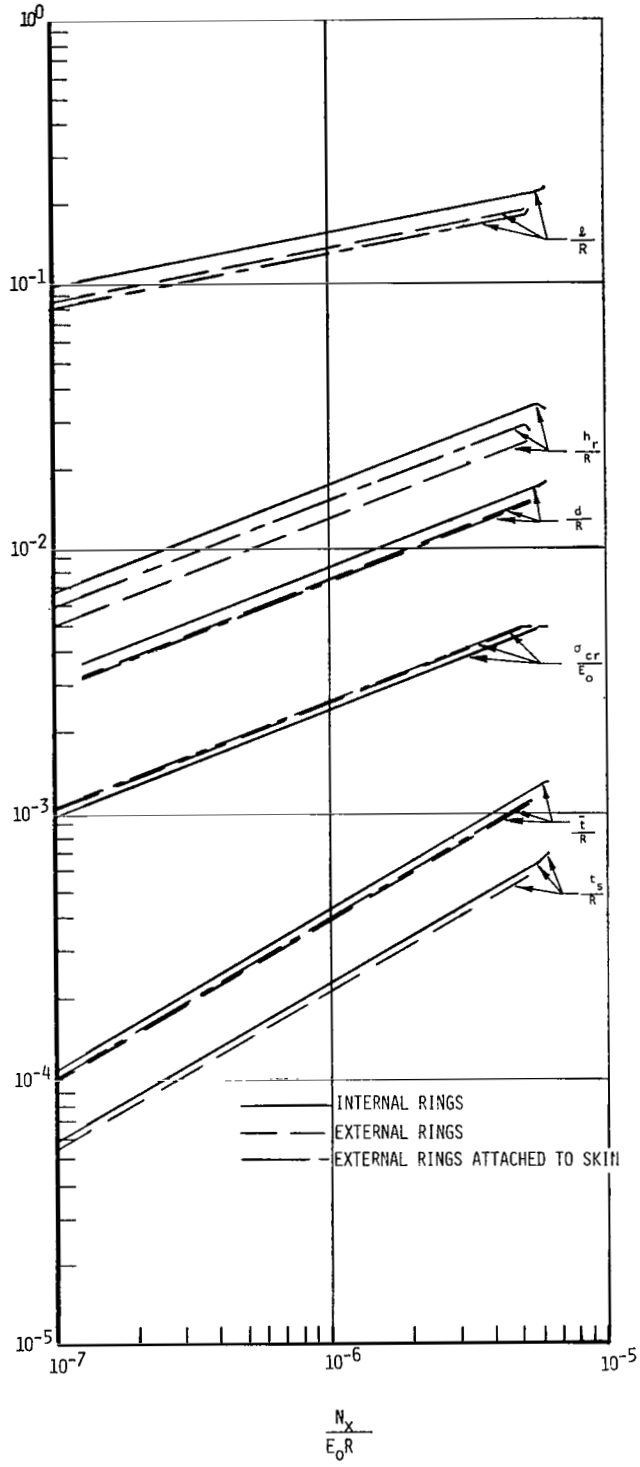

(b) External Z-stiffeners.

Figure 4.- Continued.

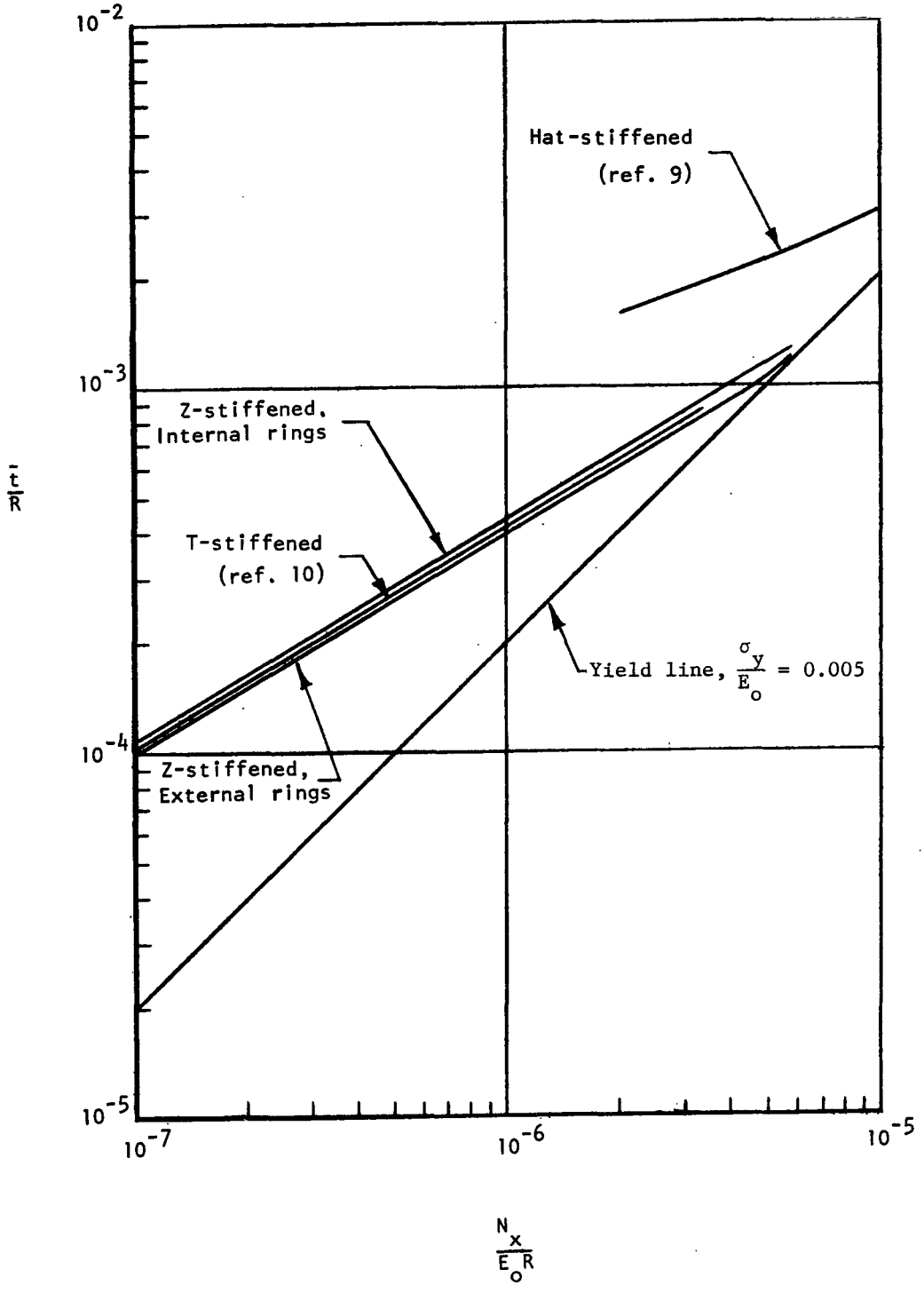

(c) Comparison of efficiency with that of other stiffened cylinders.

Figure 4.- Concluded.

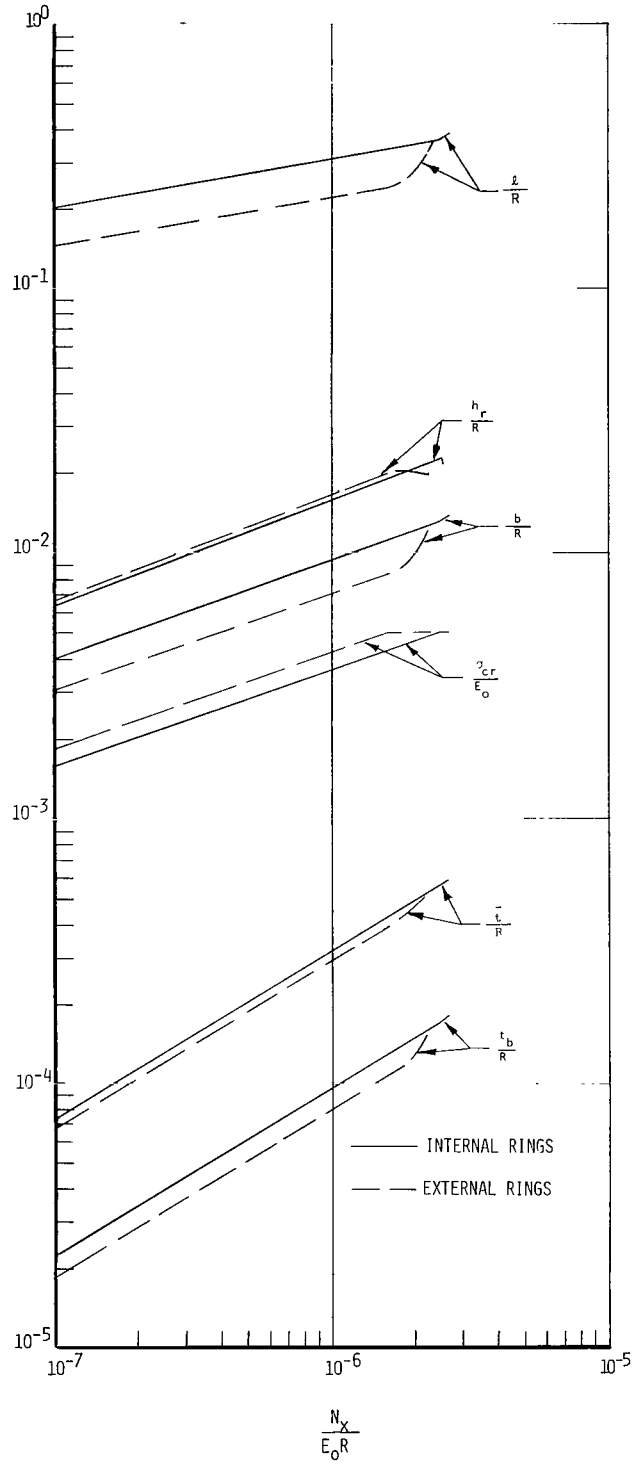

(a) Tubular.

Figure 5.- Double bead.

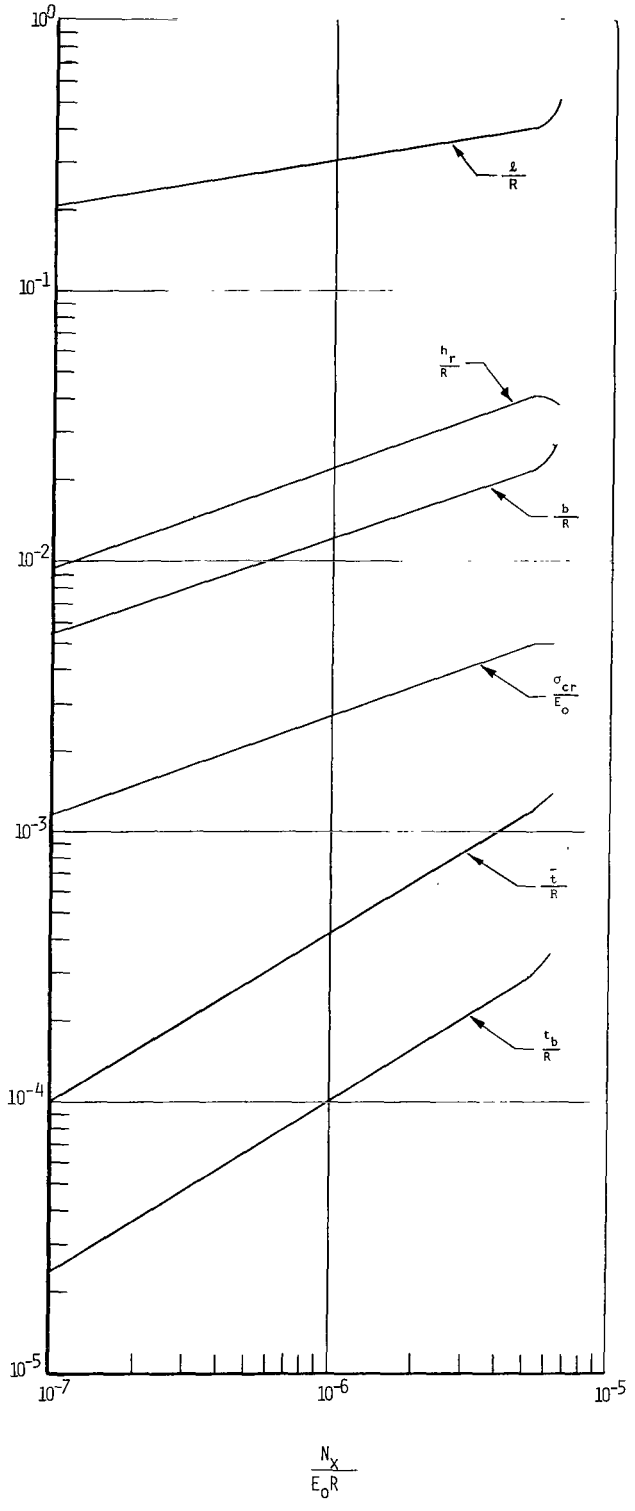

(b) Nonsymmetric internal rings.

Figure 5.- Concluded.

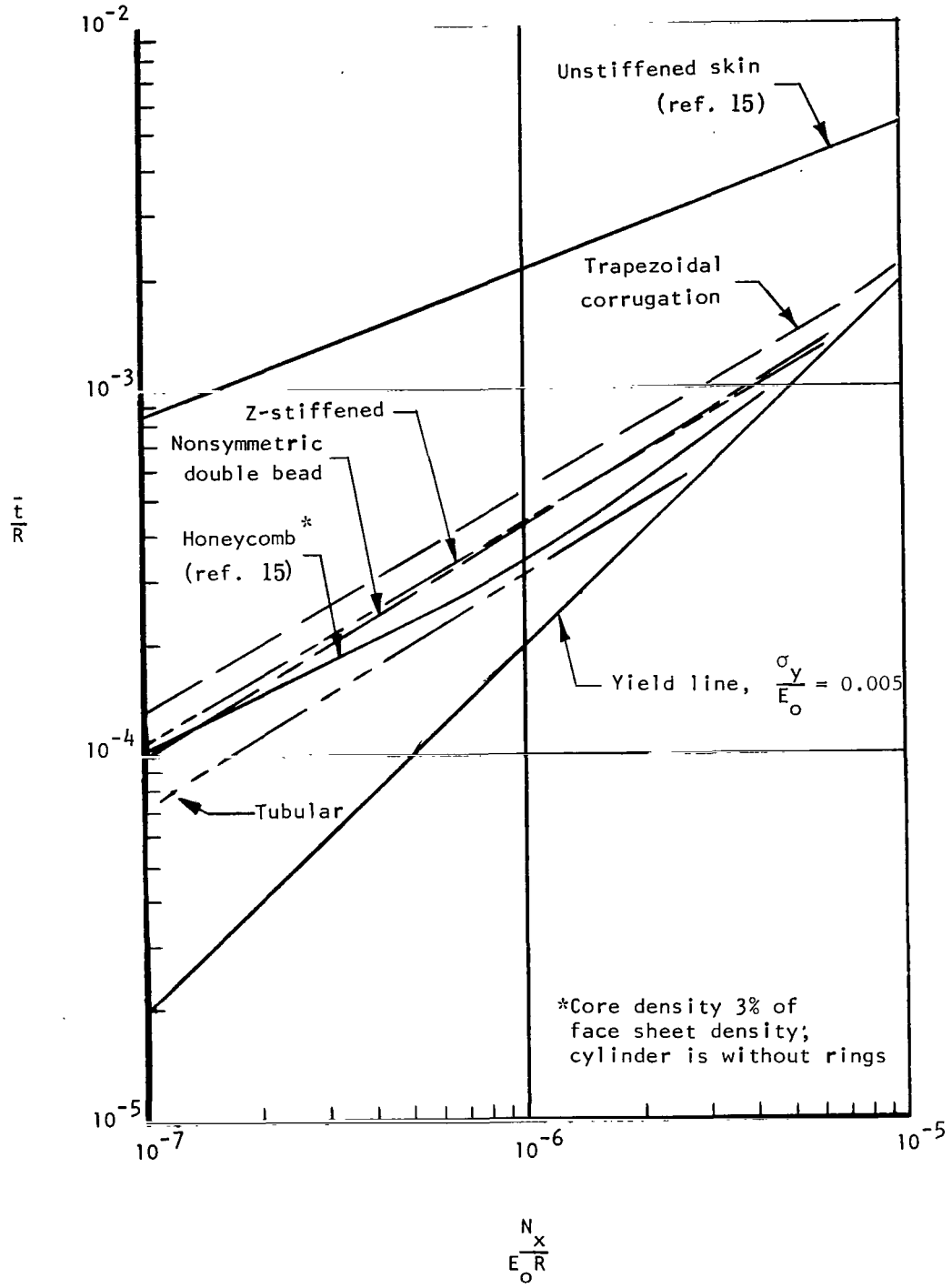

(a) Internal rings.

Figure 6.- Comparison of configurations.

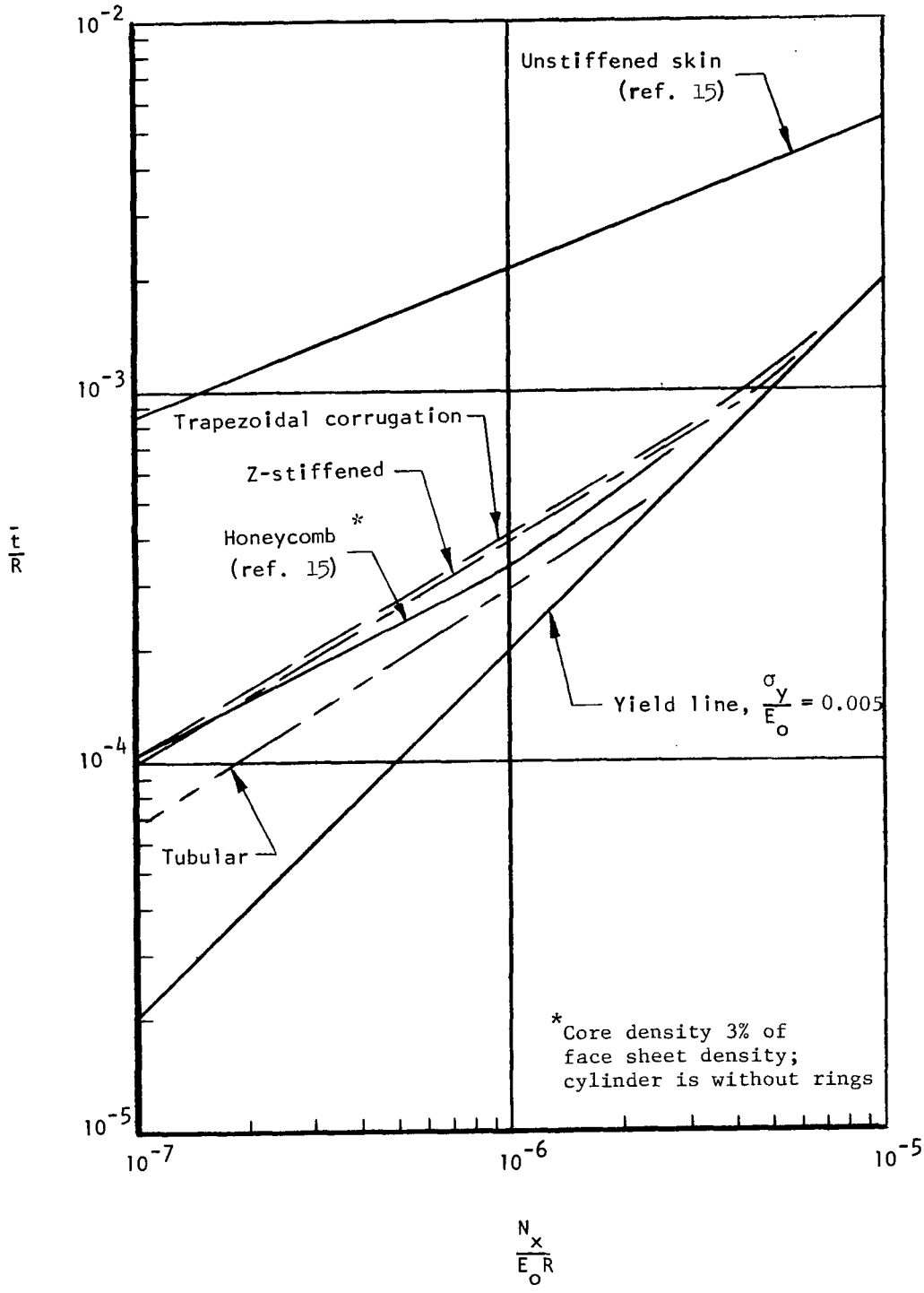

(b) External rings.

Figure 6.- Concluded.

NASA-Langley, 1972 —— 32 L-7060

"The aeronautical and space activities of the United States shall be conducted so as to contribute . . . to the expansion of human knowledge of phenomena in the atmosphere and space. The Administration shall provide for the widest practicable and appropriate dissemination of information concerning its activities and the results thereof."

—NATIONAL AERONAUTICS AND SPACE ACT OF 1958

NASA SCIENTIFIC AND TECHNICAL PUBLICATIONS

TECHNICAL REPORTS: Scientific and technical information considered important, complete, and a lasting contribution to existing knowledge.

TECHNICAL NOTES: Information less broad in scope but nevertheless of importance as a contribution to existing knowledge.

TECHNICAL MEMORANDUMS: Information receiving limited distribution because of preliminary data, security classification, or other reasons.

CONTRACTOR REPORTS: Scientific and technical information generated under a NASA contract or grant and considered an important contribution to existing knowledge.

TECHNICAL TRANSLATIONS: Information published in a foreign language considered to merit NASA distribution in English.

SPECIAL PUBLICATIONS: Information derived from or of value to NASA activities. Publications include conference proceedings, monographs, data compilations, handbooks, sourcebooks, and special bibliographies.

TECHNOLOGY UTILIZATION PUBLICATIONS: Information on technology used by NASA that may be of particular interest in commercial and other non-aerospace applications. Publications include Tech Briefs, Technology Utilization Reports and Technology Surveys.

Details on the availability of these publications may be obtained from:

SCIENTIFIC AND TECHNICAL INFORMATION OFFICE

NATIONAL AERONAUTICS AND SPACE ADMINISTRATION

Washington, D.C. 20546